Part 1

Sediments and morphology in shelf and coastal systems

Int. Assoc. Sedimentol. Spec. Publ. (2012) **44**, 1–28

Optimal use of multibeam technology in the study of shelf morphodynamics

JOHN E. HUGHES CLARKE

Department of Geodesy and Geomatics Engineering, University of New Brunswick, Canada (E-mail: jhc@omg.unb.ca)

ABSTRACT

Many of the recent advances in our understanding of sedimentary processes on the continental shelf have come about as a result of the use of multibeam sonar systems. These systems provide wide area coverage of seafloor variations in bathymetry and backscatter at typical horizontal resolutions as small as $\sim$ 2% of the water depth. The narrowest beam systems now provide backscatter data at resolutions approaching towed sidescan sonar while simultaneously providing co-registered, equivalent-resolution topography.

Even more valuable than the static view of the seabed is an ability, through resurvey, to monitor temporal variations in the seabed. By adding the time dimension, insights can be provided into the sedimentary processes rather than just the resulting sediment distribution. To achieve this, however, requires particular attention to be placed on the limitations of these survey systems, which affect repeatable accuracy. To assess the total achievable accuracy one needs to account for all the integrated components of the survey system.

In this paper, the contributions of the various sources of systematic bathymetric and backscatter error within a typical shelf multibeam survey are described. To optimize the bathymetric data, strategies for dealing with imperfections in tidal models and knowledge of the sound speed structure are described. In order to improve the backscatter data, strategies for predicting the combined effect of beam pattern residuals and the seabed angular response are detailed.

To illustrate a typical result, a pair of overlapping surveys employing widely differing source sensor resolution and accuracy is combined to try to predict the relative importance of active and relict shelf morphodynamic processes.

Keywords: Multibeam, multi-sensor integration, calibration, backscatter reduction.

INTRODUCTION

Routine application of multibeam sonar bathymetry and backscatter has revolutionized our understanding of continental shelf morphodynamics. The ability to view a near-continuous topographic surface together with variations in seabed backscatter strength provides an overview analogous to aerial photography, resulting in a vastly improved ability to interpret the seafloor sedimentary processes (Hughes Clarke *et al.*, 1996).

One of the most immediate results of this new technology has been the recognition, for the first time, of the continuity and juxtaposition of long wavelength features such as drowned beach ridges and reefs (e.g. Gardner *et al.*, 2005), or moraine complexes (e.g. Todd *et al.*, 1999). But the real challenge to maximizing the usefulness of this data will lie in the finer details revealed. The detail is in the shorter wavelength morphology that lies close to the limits of resolution of these systems.

After the first pass interpretation of the current state of the shelves, future research will be increasingly focused on monitoring their temporal evolution. The first view provides a snapshot. That snapshot allows inferences to be made about likely sedimentary processes. However, proof of the activity of those processes awaits repetitive surveying. Proof that the seabed has changed requires confidence in the absolute accuracy of both the bathymetric and backscatter output of the integrated sonar system.

Obvious change, such as new slide scars (Brucker *et al.*, 2007), overprinted iceberg scours

(Sonnichsen *et al.*, 2005), freshly emplaced debris flows (Kammerer *et al.*, 1998) or significantly-migrated bedform positions (Duffy and Hughes Clarke, 2005) can be discerned from imperfect data. However, more subtle transitions, such as accretion of thin sand sheets, deflation of near shore sand bodies, deepening of pockmarks or migration of ripples requires a level of absolute accuracy that lie at the limit of many of the integrated systems.

This paper explores the resolution and accuracy capabilities in both bathymetry and backscatter that is realistically available from currently state-of-the-art multibeam sonar systems. Practical examples are provided, illustrating the advantages and limitations of this sort of data for shelf morphodynamic research.

BATHYMETRY

Resolution

The power of a multibeam system lies in its ability to resolve sedimentary structures at wavelengths small enough to infer the processes active. Many of the sediment transport mechanisms can be inferred from the short wavelength relief. Most notably, bedforms, such as transverse dunes or ripples and longitudinal ribbons provide a clear indication of active sediment transport. Similarly, erosional scour and pockmarks are indicative of modern or relict sedimentary processes. However, such features, which have spatial scales of decimetres to a few tens of metres, often lie at the limit of the spatial resolution of the system. In the case of surface hull-mounted sonars, the resolution decays roughly linearly with depth. However, the question needs to be asked: does the disappearance of a specific short wavelength morphology with depth indicate a change in sedimentary environment, or merely a defocusing of the instrument over increasing range?

Sedimentologists wishing to conduct multibeam surveys may not have the luxury of choice of system due to logistical or financial constraints. When interpreting the available data, however, it is important to establish the achievable resolution of the utilized specific sonar system. To this end, there are a number of components that need to be considered, including:

Beam width, spacing and detection algorithm

Sonar systems are routinely quoted with beam width dimensions. Such dimensions need to be specified in two directions (Fig. 1A), along track (controlled by the transmit beam width) and across track (controlled by the receive beam width) as they may differ (Miller *et al.*, 1997).

In order to appreciate the potential of the beam footprint, its solid angle needs to be projected to the seabed over the range of depths and angles used. It is readily apparent that the minimum, resolvable dimension is strongly linked to the size of this footprint (Fig. 2). Resolution needs to be described separately for along and across track.

For an amplitude detection (deMoustier, 1993), the resolvable dimension cannot be smaller than this footprint as the echo is integrated over that dimension. Few sonars today, however, still use amplitude detection outside the near nadir or near specular region. Phase detection using a split aperture (deMoustier, 1993), in which the elevation angle within the beam footprint is defined by phase rather than peak intensity, is almost universally used. In this manner, discrimination across track can be achieved based on phase (Fig. 1C). For the long, lower grazing angle echoes, phase (and thus feature definition) can be discerned at a scale significantly finer than the beam footprint dimension (Hughes Clarke *et al.*, 1998). For most sonars this is achieved by having beam spacings across track that are tighter than the beam footprint dimension. The most common example of this is the "Equi-Distant" beam spacing (EDBS) mode (Fig. 1B) increasingly offered. For conventional phase detection, each beam still has only one depth solution (what is termed the "zero phase crossing, solution 0 in Fig. 1C), but it is based on just the phase slope in the central part of the beam.

Figure 2 (left; EM1000 images) illustrates the resolution achieved using equi-angular beamspacing when the EDBS philosophy is not employed. As can be seen, the definition of the boulders degrades notably as one moves to the outer part of the swath. The compromise in EDBS is that, for a finite number of beams, the beam spacing in the near nadir region has to be compromised to accommodate the extra solutions at lower grazing angles (see beam spacing in Fig. 1B). For example for the EM1002, which has 111 beams over a 150° sector, in equi-angular mode (EABS) the near nadir beams are spaced at 1.35°, whereas in EDBS they are spaced at 3.84° (resulting in lower nadir resolution and wider than the 2° beam width, resulting in corrupted backscatter data).

Most recently, the limitation of EDBS has been removed through the use of "high definition" beam

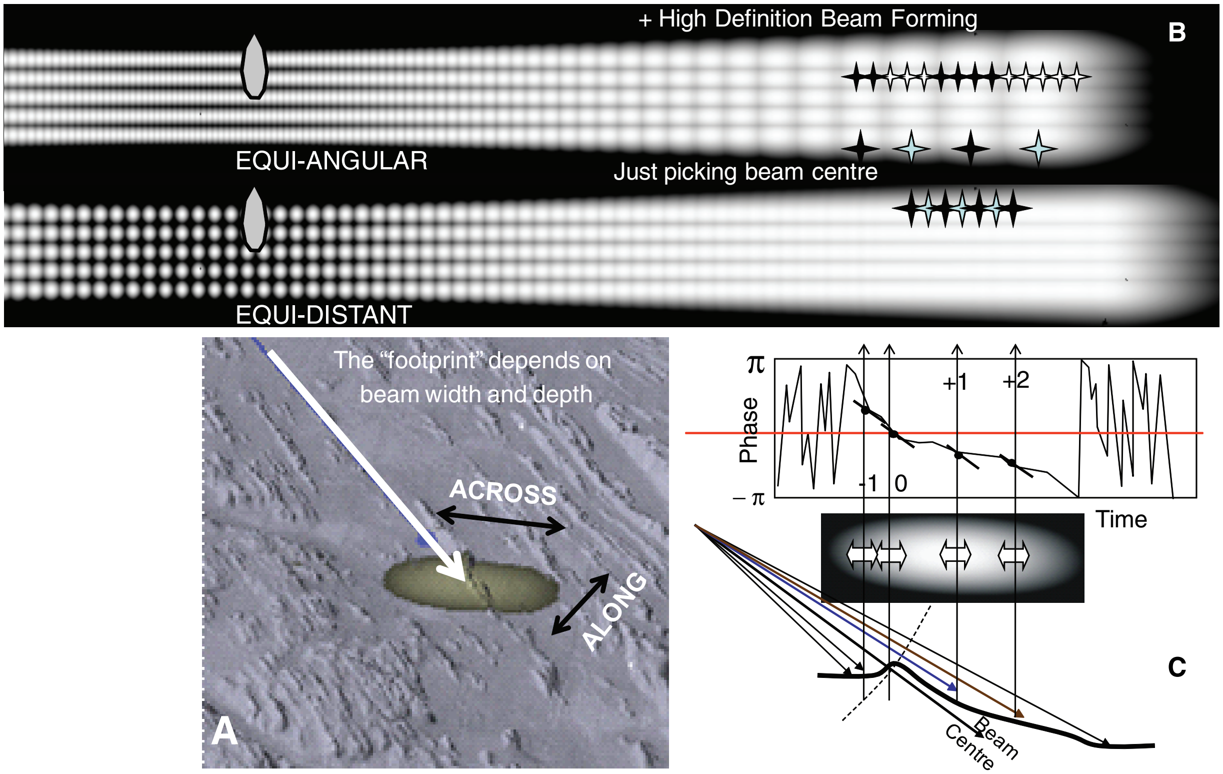

Fig. 1. (A) Representation of an oblique narrow beam footprint on a typical seabed terrain. (B) Variation of size and spacing of a series of multibeam profiles, comparing and contrasting the bottom detection solution (represented by stars alternating black and white from beam to beam) spacing offered by equi-angle, equi-distant and high density beam forming (multiple solutions per beam). (C) The method of describing the across-track relief within a single beam footprint by looking at the evolution of differential phase over the across-track beam dimension. For this method, the centre of the beam corresponds to the point at which the differential phase is zero. For conventional detection, this point is the only one located (by regression through the phase slope), whereas for high definition, multiple points on the phase curve (corresponding to multiple angles with respect to the beam centre) are identified.

forming (Kongsberg, 2005) in which, for phase detection, multiple points on the phase slope are used within a single beam footprint (Fig. 1C, solutions −1, +1 and +2). The physical beam spacing is actually equi-angular, but more depth solutions than beams are generated by subdividing the lower grazing angle beams. This gets around the compromise in conventional EDBS as optimal beam spacing for amplitude detection is retained.

However tight the beam spacing in the across track dimension, in the along track direction, the beam dimension and its spacing will still limit resolution. Thus narrower transmit beam widths are to be favoured. For a given transmit beam width and depth, the fore-aft dimension of the footprint grows with obliquity. Thus for geological purposes, resolution will generally decay away from the nadir region. Again it is important that this limitation be noted when interpreting the distribution of features close to the limit of resolution such as ripples or boulders.

There is a wide variety of multibeam sonars available, but the ones most commonly used on the continental shelf are those in the ~100 kHz range. The EM1000, operating at 95 kHz with a beam width of 2.4° × 3.3°, first appeared in 1992 and has been used extensively in continental shelf surveys worldwide. Large tracks of the US conterminous continental shelf have been covered with this sonar (Gardner *et al.*, 2005, Valentine, 2005, Butman *et al.*, 2006). The RESON 8111 (100 kHz, 1.5° × 1.5°) appeared in ~ 1996 and has been used commercially for similar scale continental shelf mapping (Wilson *et al.*, 2005, Intelmann *et al.*, 2006). The EM1000 was superseded by the very similar but higher resolution EM1002 (2.0° × 2.0°) in 1998, but many were still used until ~ 2005. The EM1002 has been employed on a regional scale for

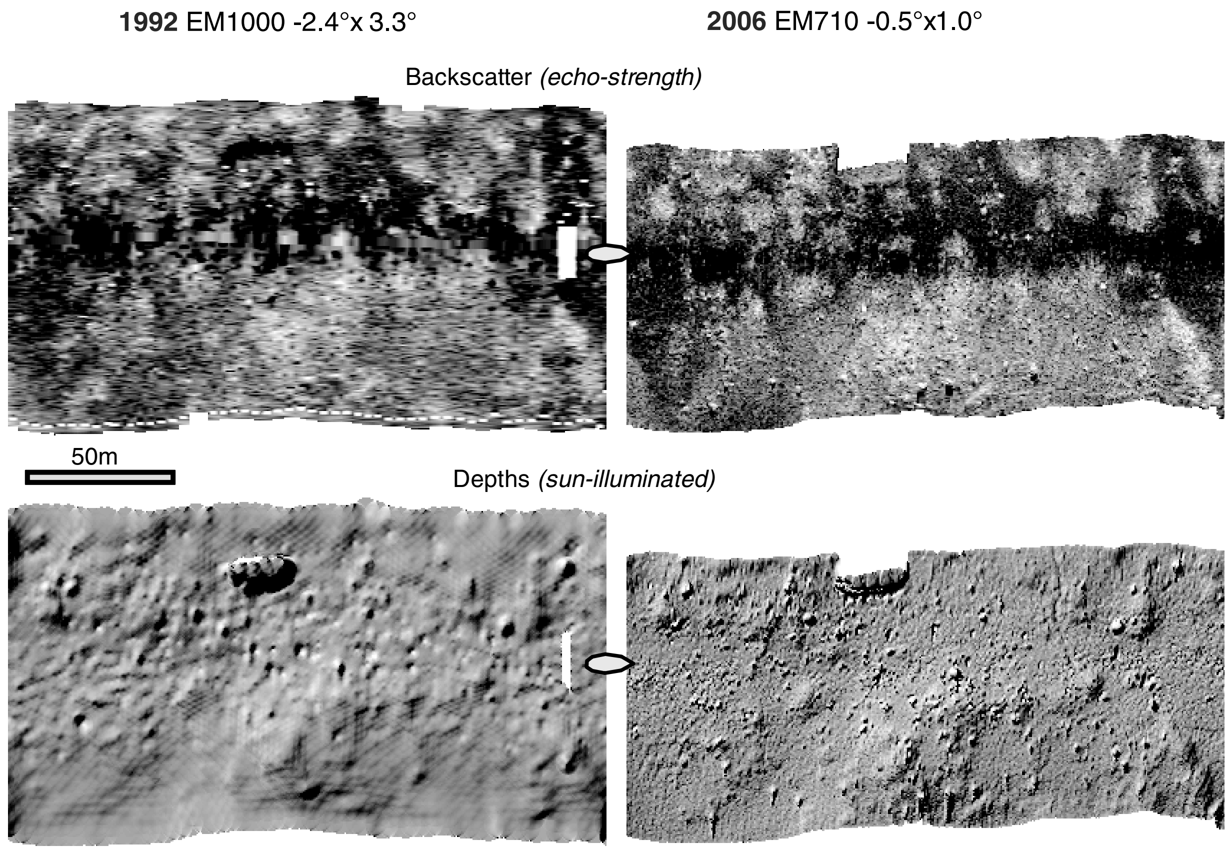

Fig. 2. Comparison of the backscatter and bathymetric imaging resolution of two generations of common multibeam sonar systems. Wrecks and boulder fields in 25–40 m of water. Note the increased definition in both bathymetry and backscatter imaging of the boulder targets. Note also the pronounced drop in resolution for the outermost beams in the case of the equi-angle beam spacing utilized by the EM1000. Beam widths are given for both scanners.

continental shelf geological mapping by Canadian agencies (Pickrill & Todd, 2002, Conway *et al.*, 2004). The EM710 (Fig. 2, right hand side images) represents one example of the next generation of sonar systems that are replacing the 1000/1002 series with beamwidths now as narrow as $0.5° \times 1.0°$, and for the first time include yaw stabilization. The practical examples here compare and contrast the EM1000 and EM710 sonars.

Roll, pitch and yaw stabilization

In order to optimize the resolution, the sounding density along track should be as high and as even as possible. Ping rate for single ping systems is controlled by the two way travel time (TWTT) to the outermost beams. The wider the angular sector, the lower the ping rate. Thus for a given speed, resolution will decay with sector width resulting in a competition between lateral coverage and resolution. This is starting to be solved with the recent use of multiple swaths per ping cycle system. This is now offered (but only delivered in July 2008) by a number of manufacturers and promises to improve this limitation.

Irrespective of the along track vessel movement between pings, the outermost beams may be displaced more or less depending on the vessel rotations and the form of stabilization (Fig. 3). Roll stabilization is essential if the full swath is to be used, but does not affect the along track density. Pitch stabilization is more important in deeper water. But the biggest issue in continental shelf depths is yaw. In a cross-sea, vessel heading is hard to maintain, and as the water depth becomes shallower the helmsman is forced to take stronger corrective action to maintain minimal survey line offset. The requirement for yaw stabilization depends on the inter-ping yaw shift and the transmit beam width. As narrow transmit beams are

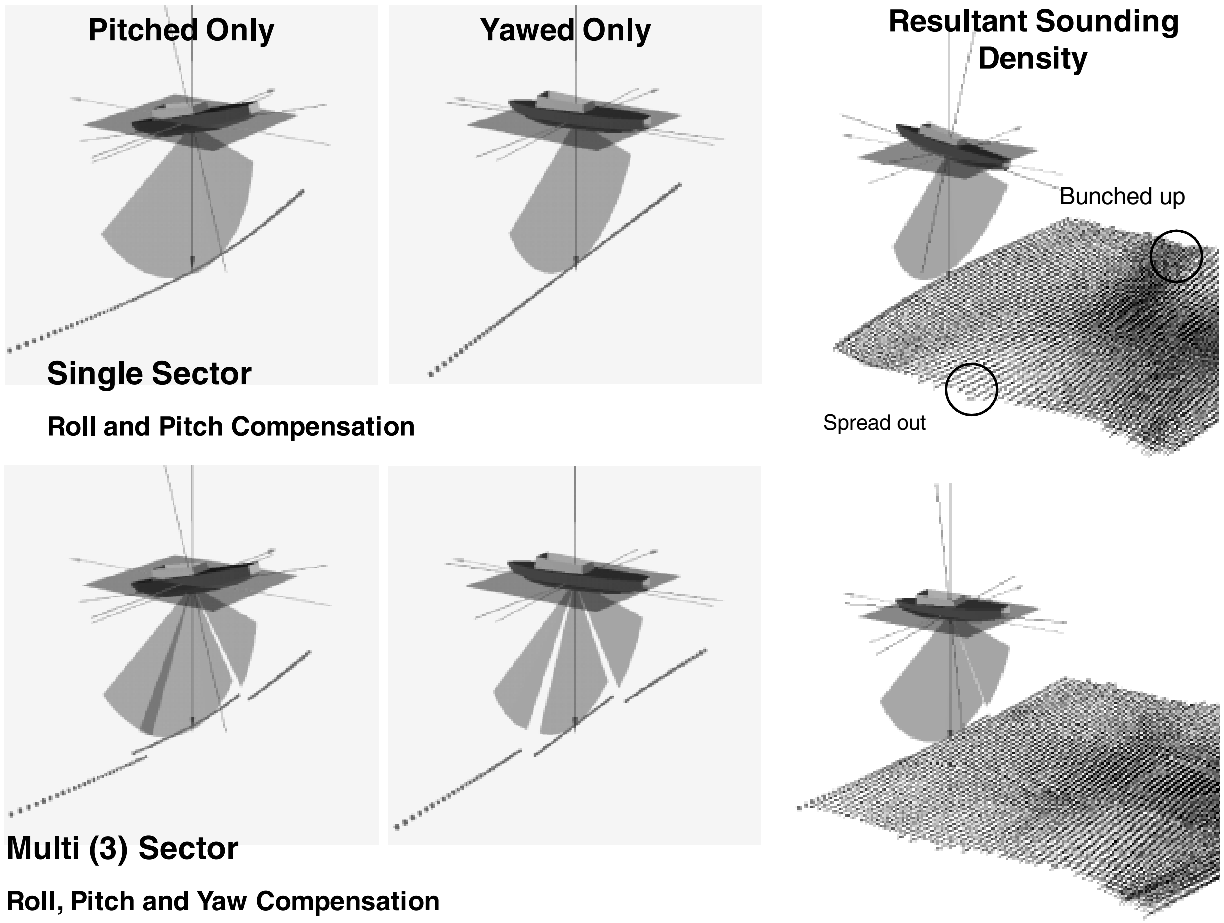

Fig. 3. The strategy and result of active roll, pitch, and yaw stabilization. Note particularly the improvement in even sounding density achieved by using the multi-sector strategy. This strongly impacts on the ability to maintain resolution for all regions ensonified.

being used to increase resolution, the requirement for yaw stabilization is increasing.

To achieve yaw stabilization requires the use of multiple sectors (Fig. 3). For a single sector system, the full swath is illuminated using a single broad transmit beam that can only utilize a single steering angle, which must be chosen as a compromise whereby both sides of the swath are aligned as best as possible. For the case of multiple sectors, a succession of individual transmissions is generated, closely spaced in time (separated in time only by the length of each pulse). Each sector/transmission addresses only a specific subset of the total swath and can thus have a unique steering angle that best aligns that subset of the swath. In this manner the compromise inherent in single sector systems can be avoided, allowing yaw stabilization that requires, as a minimum, opposite-sense steering angles for each side. Without yaw stabilization, there will be zones of lower sounding density (on the outside of shallow corners; Fig. 3) where the target resolution, and thus geological interpretation, is compromised.

Accuracy

Achievable resolution is no guarantee of absolute survey accuracy at that level. Any survey consists of a series of systematically offset corridors of data, normally called swaths. The combination of multiple swaths requires a common reference datum. Absolute accuracy limits will corrupt the data in two ways: (1) when blending the overlap, the view of the seabed in the region of overlap will be defocused; and (2) when comparing the swath with data collected at other times, only scales of seabed change larger than the combination of the achievable accuracies of both surveys will be discernable.

While manufacturers' brochures tend to emphasize the sonar-relative range and angle accuracy, these usually input an uncorrelated random noise in the sounding data rather than a systematic bias. For operations where repeat surveys are required for sedimentary change assessment, it will be the systematic errors that are more important as they will generate biases that can be confused with true sediment accretion or deflation. There are a number of components in addition to the sonar range and angle measurement that contribute to the achievable degree of accuracy.

Positioning systems – horizontal

Positioning requirements are normally quite different for horizontal and vertical. The Global Positioning System is now used universally for the horizontal component of marine surface surveys. The achievable accuracy depends on the type of GPS chosen. Stand alone versions (non-differential) will allow 10–15 m accuracy, sufficient for deep-sea operations (where the resolution is below this), but not for shelf investigations where some form of differential GPS will be required.

Differential corrections from a coastal (usually Coastguard) service will provide sub-2 m horizontal accuracy, adequate for outer continental shelf surveys. To obtain better accuracy than this would require an interpolated correction service, such as Fugro OmniSTAR (Visser, 2007) or C&C CNav (Chance *et al.*, 2003), often referred to as Globally-corrected GPS (GcGPS). Such services provide decimetre level horizontally, meeting practically all the needs of shelf and inshore surveys.

To get to a centimetric level positioning requires a local base station and "Kinematic GPS" (USACE, 2002). This is not practically needed for horizontal positioning but, as outlined below does provide the necessary level of vertical positioning to account fully for tides and squat.

Assuming that the horizontal accuracy of the positioning system meets the needs of the seabed change detection requirement, one still has to ensure proper integration of that position. The most common issue is one of time delays between sonar and positioning sensor clocks. Delays will result in systematic, along survey-line displacement of the swaths of data. This will generate apparent migration of seabed features that could be confused with real change. Detection of such offsets is normally quite easy by comparing the displacement of linear targets such as bedrock outcrop ridges or sand wave crests within a single survey.

Angular measurements – accuracy and alignment

All sonar relative ranges and bearing need to be adjusted for array orientation at transmit and receive operations. Generally the stated angular accuracies ($<0.05°$) of the high-end GPS-integrated inertial motion sensors are more than adequate for the accuracy levels needed for operations. However, it is not the instrument accuracy that most concern us, but rather the integration of sensor data. Proper integration requires knowledge of sonar to motion sensor alignment and timing calibration.

Misalignment or mistiming of sensors relative to each other can create both static biases (for example a roll bias) and dynamic residuals (so called wobbles). For a full review of the sources of dynamic motion residuals, the reader is referred to Hughes Clarke (2003). From the point of view of the sedimentologist, the effects have two end-member results. Firstly the static biases impede the ability to measure change, and secondly the dynamic motion residuals can be confused with, or obscure, real seabed terrain.

Water column sound speed structure

An integral component of an accurate depth measurement is the proper accounting of sound wave propagation and refraction in the water column (Beaudoin *et al.*, 2004). This depends on an adequate knowledge of the sound speed structure in the ocean. Failure to account for this properly will result in either a dynamic residual (Hughes Clarke, 2003) or a systematic, convex or concave across track bias (Fig. 4), the magnitude of which depends on the unmonitored changes in the water column. The water column is changing continually in time and space and thus the magnitude and sign of the error will reflect the time and/or distance that has passed since the last sound speed measurement (Hughes Clarke *et al.*, 2000). Figure 4 illustrates a typical summer continental shelf oceanographic section, illustrating the rapid change in refraction conditions from fresh water stratified, to a tidal mixed area to a thermally stratified ocean within distances of tens of kilometres.

In order to minimize the significance of sound speed errors, a variety of strategies may be developed including continuously monitoring the

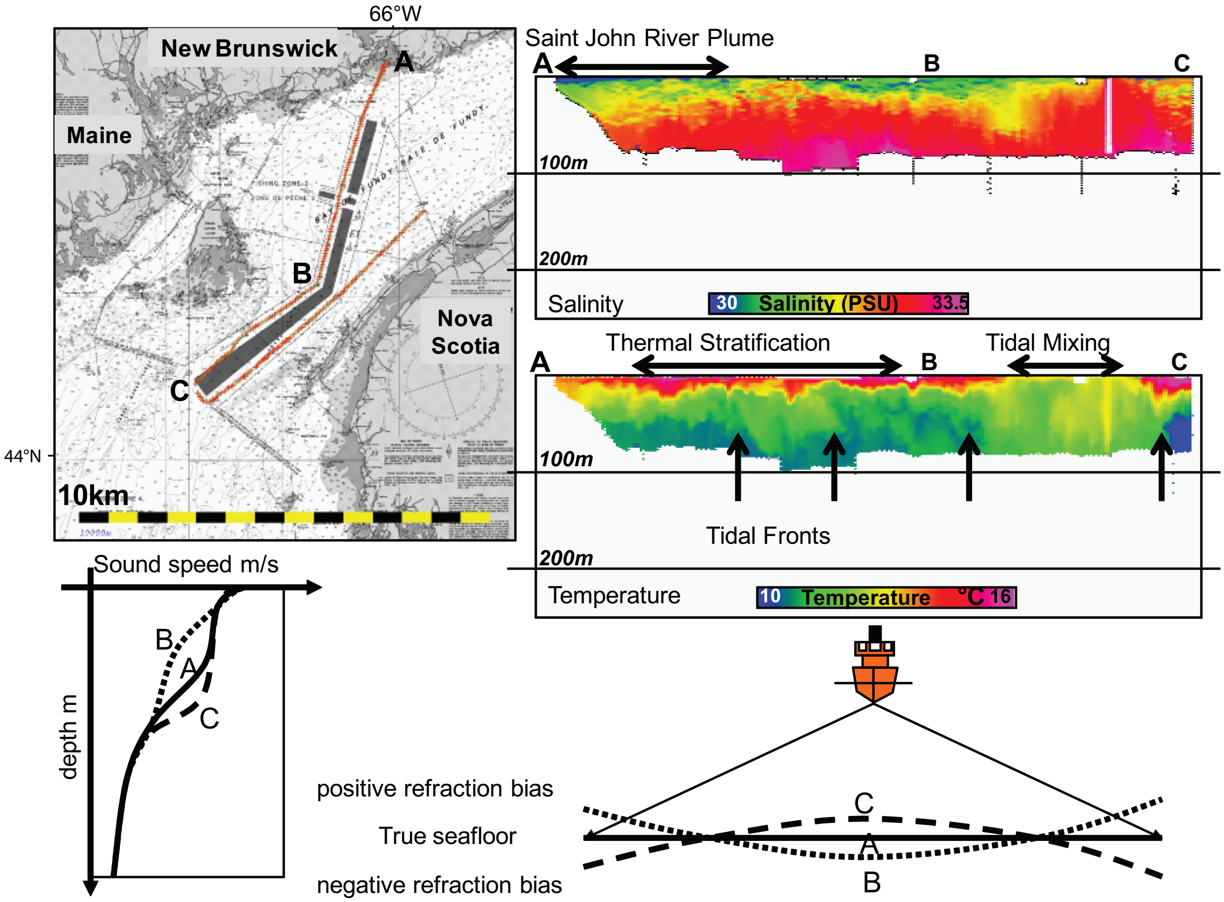

Fig. 4. Variability in the sound speed field for a typical summer-time continental shelf. Example dogleg transect illustrated from A to B to C across the Bay of Fundy. Note transition from a fresh-water stratified environment, to a thermally stratified environment, punctuated by zones of increased mixing, separated by abrupt tidal fronts, spaced at times by only a few kilometers along track. Such changes, which alter the location of the velocline, lower left, result in systematic across track biases in the resulting bathymetric data, lower right. Data were derived from a continuously operating underway profiler at 12 knots, with sample spacing of about 1 km.

sound speed (Cartwright & Hughes Clarke, 2002), reducing the angular sector of the swath, and reviewing archived information about likely water mass variability and then designing the survey to take that into account.

The illustrated profile (Fig. 4) required updated sound speed structure information at approximately half hour intervals to maintain the full $\pm$ 65° swath within IHO order 1 specifications (International Hydrographic Organization, 1998). Such a profiling frequency is not practical unless underway profiling strategies are available. Prior knowledge of this oceanographic variability would allow the prudent user to break up the survey into regions of common watermass type.

In all cases, it should be appreciated that reducing the angular sector is the most reliable way of minimizing these errors. This results in a low rate of coverage, but will improve the data density (as the required maximum two-way travel time is reduced) and thus increase the resolution. A practical example is presented (Fig. 5) showing inter-survey bathymetric surface differences for Squamish Delta in Howe Sound, British Columbia. The upper delta is accreting $\sim$1 m yr^{-1} on average. The delta has been the subject of investigation with multibeam since 2004 (Brucker *et al.*, 2007). Maintaining sufficient sound speed data to survey represents a challenge due to the presence and variability of a freshwater plume emanating from the mouth of the Squamish River that is modulated over a tidal cycle.

The first difference map (Fig. 5A) shows the apparent changes based on two regional surveys

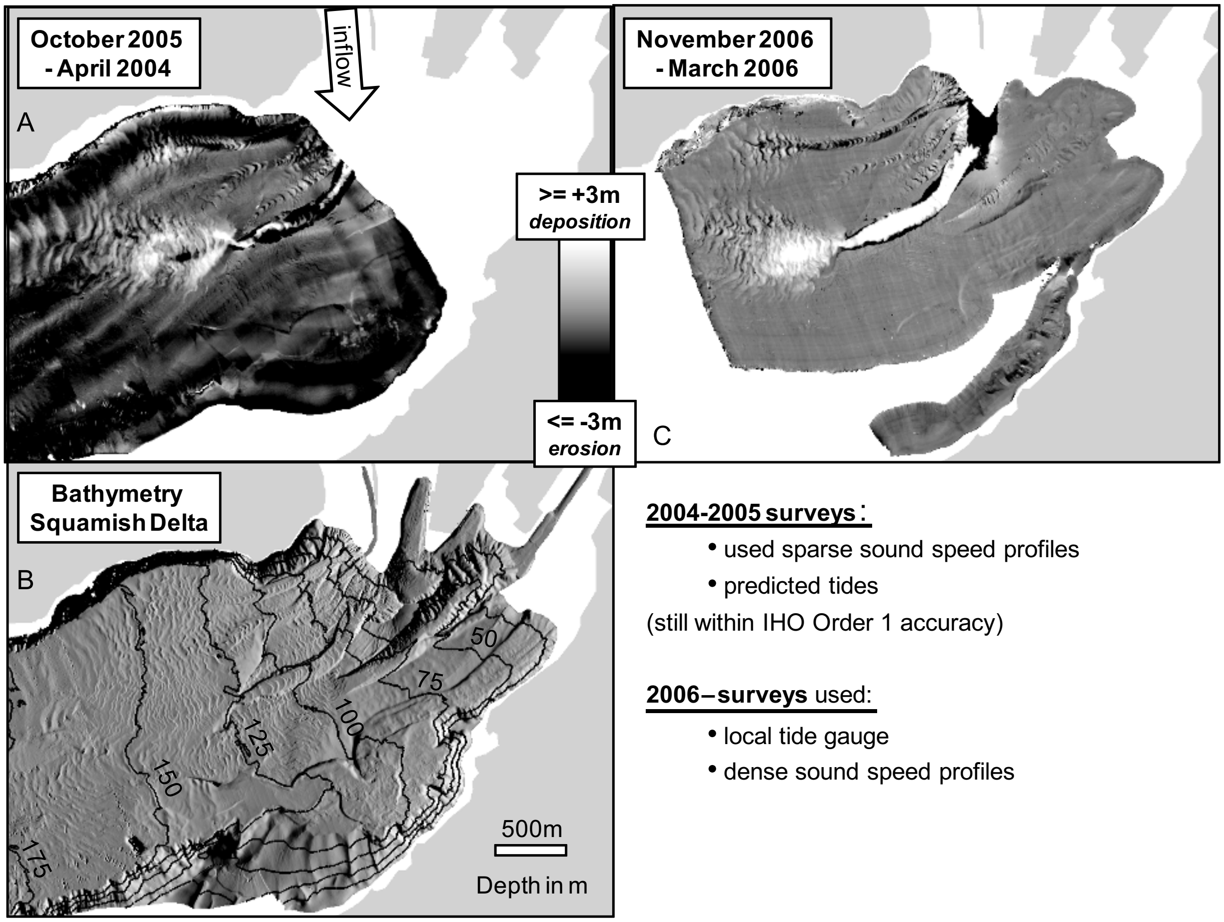

Fig. 5. Example of the effect of water column uncertainty on estimates of seafloor change. (A) difference map between two surveys (EM1002) in 50–200 m of water. (B) bathymetry of the Squamish Delta, both surveys using sparse sound speed profiles, obtained several kilometres away. (C) difference map between two surveys (EM3002). For both surveys, the greyscale used is the same between −3 m and + 3 m. Differences greater than this are thresholded to black or white.

that did not undertake extra sound speed measurements close to the river mouth. While it is immediately apparent that gross change has occurred in the delta foreset channel and on the proximal lobe to the SW, there is a conspicuous pattern of striping developed over the difference map on the rest of the delta surface that does not obviously correlate with likely depositional or erosional processes. These are a result of refraction residuals (Fig. 4D) in each survey. Note that the residuals are actually only ~ 0.5–1.5 m in 100–200 m of water which is well within International Hydrographic Organization standards, which are typically ~ ± 1.5% of water depth (International Hydrographic Organization, 1998).

By contrast, the second difference map (Fig. 5B) was obtained using much more frequent sound speed profiles collected in the local area throughout the survey. As can be seen, the striping is nearly absent (the two surveys were run orthogonally to each other and thus the contribution of each survey should be apparent). Only using these methods can one start to assess the scale of the over-bank sedimentation that contributes to the long term growth of the delta front.

Tidal reduction, measurement and models

However good all the other integrated components of the depth measurement are, ultimately the depth must be referenced to a stable vertical datum. Tidal reduction has always been a necessary step. For traditional coastal hydrographic surveys the standard has been to install a local gauge.

This approach is valid for regions in the local area that share the same phase and amplitude of the

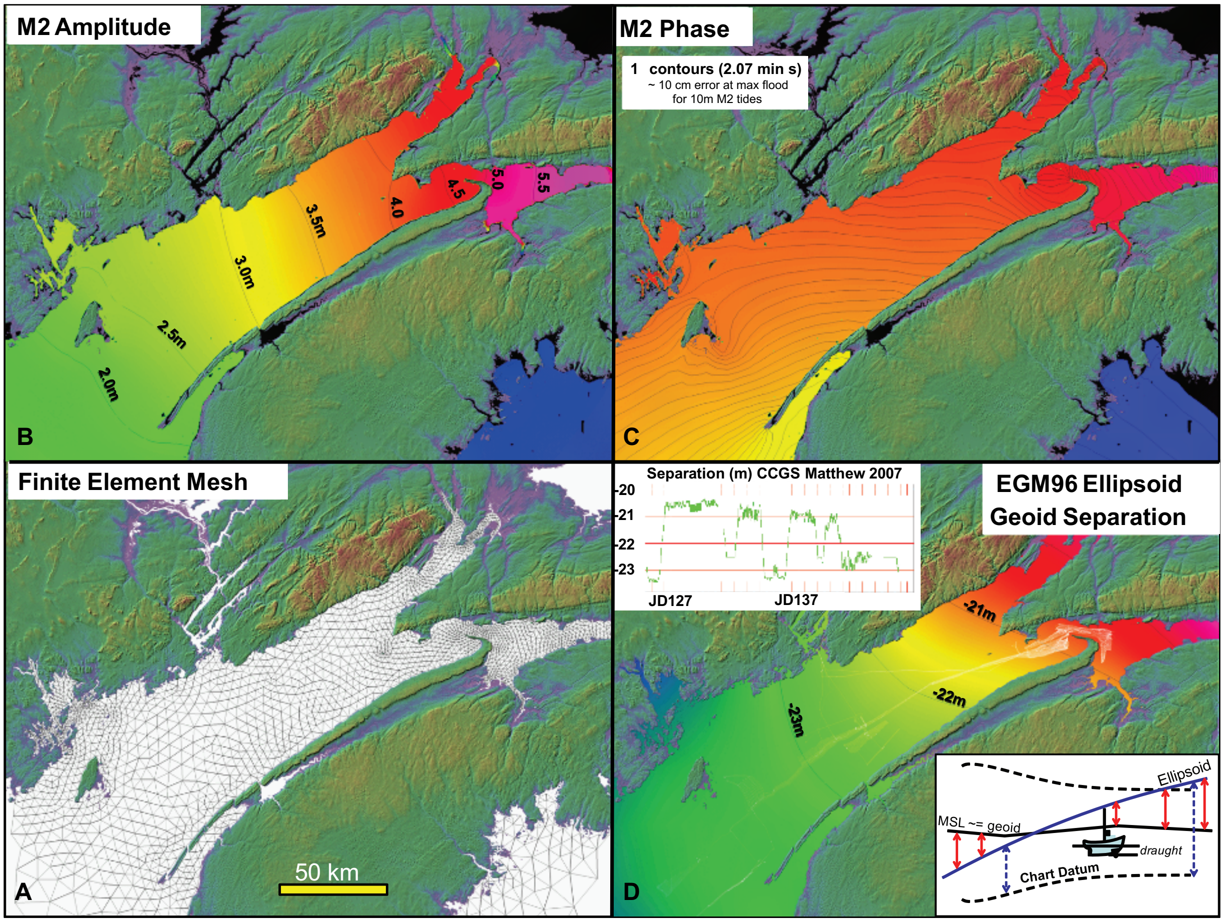

Fig. 6. (A) Resolution of the hydrodynamic model for the Bay of Fundy; (B) the resulting distribution of tidal amplitude; (C) the phase of the constituents (M2 illustrated here, but available for all of M2, S2, N2, O1, K1); (D) in order to take advantage of GPS heighting, the addition of an ellipsoid-geoid separation model is required. The profile represents the correction necessary to shift measurements from the ellipsoid to the geoid over a 20-day period of operation (the ship tracks are illustrated in D).

tide. However, as one moves along restricted coastal areas or onto the open continental shelf, knowledge is required of the propagation of the tidal wave. This is often expressed in terms of a co-tidal chart, where regions are defined in which tides at a reference station need to be scaled and delayed to be valid in adjacent regions (Admiralty, 1969). For coastal areas, this knowledge is based on historic location of tide gauges at adjacent locations along the coast. However, as one moves out onto the continental shelf, adequate tidal data are lacking. For an open coastline the propagation of the tidal wave from the edge of the continental shelf was previously poorly known. However, recent modelling, based on analysis of Topex Poseidon sea surface elevation data (e.g. Dupont *et al.*, 2002) has resulted in the development of hydrodynamic models that predict the propagation of the wave across outer-continental shelf regions. In this manner, a dynamic tidal solution may be calculated along the track of the survey vessel, appropriate for the location and time of the vessel at every point.

In Fig. 6, an example on one such model for the Bay of Fundy is presented. The model is based on the WebTide (Department of Fisheries and Oceans, 2005) hydrodynamic model, which is available for the entire Canadian continental shelf. The resolution is variable and uses a finite element triangulated network (Fig. 6A). The Bay of Fundy is a region in which the amplitude of the tide (Fig. 6B) more than doubles as one moves up the bay and the phase is successively delayed (Fig. 6C) particularly at constricted regions (Greenberg, 1979).

Of most concern are constricted regions where the tidal wave is impeded and the phase contours (Fig. 6C) are tightly spaced. In these regions, a local gauge can become invalid within a few kilometres. The model illustrated here has been adopted as the prime reference for reprocessing of multibeam surveys from 1992 to 2007 in the region. This approach was chosen over conventional tide gauges due to the problems associated with the necessity of maintaining multiple gauges and accurately defining the tide in the central bay. Disadvantages of tidal models are twofold:

1. Their accuracy offshore is hard to assess. It is generally only tested against point stations on the coast;
2. They cannot predict non-tidal sea level signatures due to, for example, atmospheric pressure variations, or wind-driven sea surface run up.

In the event of there being an unmodelled amplitude or phase error in the applied tidal profile, it will not be immediately apparent if sequential survey lines are just a few tens of minutes apart. This is because the magnitude and sign of the residual error will change only with periods similar to the tidal forcing. But if a pair of lines is run with a time gap between them of several hours (more strictly with a significant change in tidal phase) then the sign and magnitude of the tidal residual error is unlikely to be the same.

Figure 7 illustrates the analysis of a repeat survey on the continental shelf in which the inter-survey differences are clearly dominated by the tidal signature. Two types of residual are seen. Gradually changing magnitude and sign of the difference across the survey progression indicate either a phase or amplitude error in the tide. Abrupt steps in the sign of the difference along a shiptrack indicate that the survey has been broken for an unspecified period. Only the second type of error will show up in the short wavelength morphology as an abrupt inter-line step. The first type of error, results in only a few centimetres difference in the error between adjacent lines (even though both are actually wrong). The example in Fig. 7 is of two surveys, one day apart and using an identical platform just using orthogonal survey line orientations. As most of the error sources cancelled out, the inter-survey bias was minimal (1 cm), but the tidal errors are seen to be the dominant signature even though the tide gauge was only 10 km away. Both Fig. 7 and Fig. 5A illustrate that it is important to know the survey line orientation when examining surface difference maps. Any apparent lineation that is parallel to one of the two survey line orientations should be treated with suspicion. If a certain sedimentary process that has a preferred grain is suspected, the survey lines should be oriented so that any systematic biases would not be confused with the natural process of interest.

As the magnitude and sign of the tidal error only change over periods of hours, a strategy of avoiding long survey lines that only generate overlap after several hours should be adopted, thereby minimizing interline errors. The preferred sequence would be to break up large areas into several regions with line lengths no more than about an hour. Note that the error is still present but is not manifested as abrupt line to line mismatches. This provides a much clearer view of the geomorphology. Steps will still be generated at survey region boundaries. Similarly survey strategies that involve "race track" strategies, where alternate lines are run with fill in lines at other phases of the tides are to be avoided. This is often implemented for vessels that have a large turning radius compared with the line spacing.

Note that this strategy of breaking up large areas into smaller sub-regions is actually complementary to the aim of minimizing water mass variability as the data collected are within a similar water mass, and sound speed sampling strategies can be designed around a shifting box survey region. An increasingly-used alternative to the tidal measurement and modelled interpolation is to use a GPS-derived ellipsoid height. Conventional differential GPS heights are in the $\pm$ 5 m vertical accuracy range and thus of no value. Kinematic GPS offers the best solution but are limited by separation of platform and base station (generally to less than 20 km, USACE, 2002).

An emerging approach involves the GcGPS services such as C-Nav or OmniSTAR which offer a vertical accuracy of several decimetres. With smoothing, this provides an adequate result for tidal correction in continental shelf waters where one is beyond the practical range of kinematic GPS and the tidal propagation models are uncertain. The major problem with these services is reliability (Hughes Clarke *et al.*, 2005). The vertical profile needs to be filtered and edited to account for discontinuities and interruptions.

Before any ellipsoid height model can be used, the separation between that surface and the desired reference vertical datum (usually either Chart

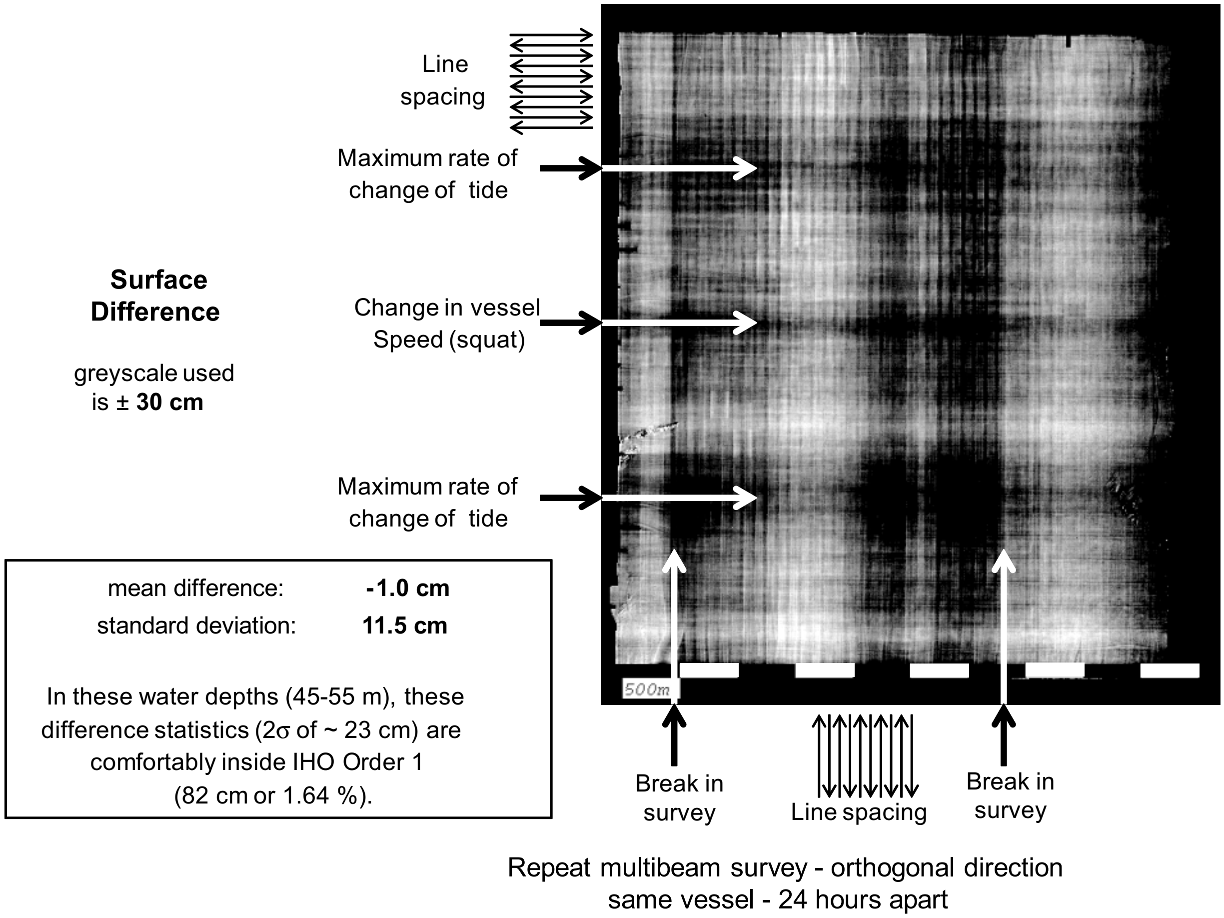

Fig. 7. Map of inter-survey differences for two EM1002 survey performed 24 hours apart. The region is an extremely low relief sand seafloor in the English Channel. Two rock outcrops can be seen on either side of the map. They appear as a disturbance in the difference map due to slight timing and bottom tracking uncertainty. There was no real change in the seafloor between the surveys, yet the difference map illustrates that the inter-survey errors are not random. Rather they are dominated by imperfections in the tidal model. Such patterns need to be understood before any real sedimentary change can be interpreted.

Datum or Mean Sea Level) needs to be established. For a small area (less than a few kilometres) a single shift can often be applied, but typical geoid-ellipsoid surface slopes are in the 3 to 10 $\mathrm{cm\,km^{-1}}$ range and thus for continental shelf areas, one needs to have a model of the geographic variation in the separation. Figure 6D illustrates the EGM96 (Lemoine *et al.*, 1998) ellipsoid to geoid surface separation used for the Bay of Fundy. The superimposed ship tracks run several hundred kilometres up and down the bay and thus require a continuously varying separation to be applied to the data (profile inset in Fig. 6D). In this manner repeat surveys may be conducted and referenced to a stable datum (the ellipsoid) wherein one can start to estimate sedimentary change at a vertical scale of a few decimetres.

BACKSCATTER

Increasingly, spatial variations in the seabed backscatter strength are being used as an additional tool to aid in interpretation of shelf sedimentary processes. In order to use this effectively, a proper understanding of both the physical controls on seabed scattering and the effect of sonar radiometric and geometric imaging is required.

Physical controls on seabed scattering

Seabed backscatter strength is driven by the seabed's physical properties (Jackson *et al.*, 1986) and thus is potentially a useful indicator of sedimentary environment. A direct correlation between acoustic backscatter strength and a simple

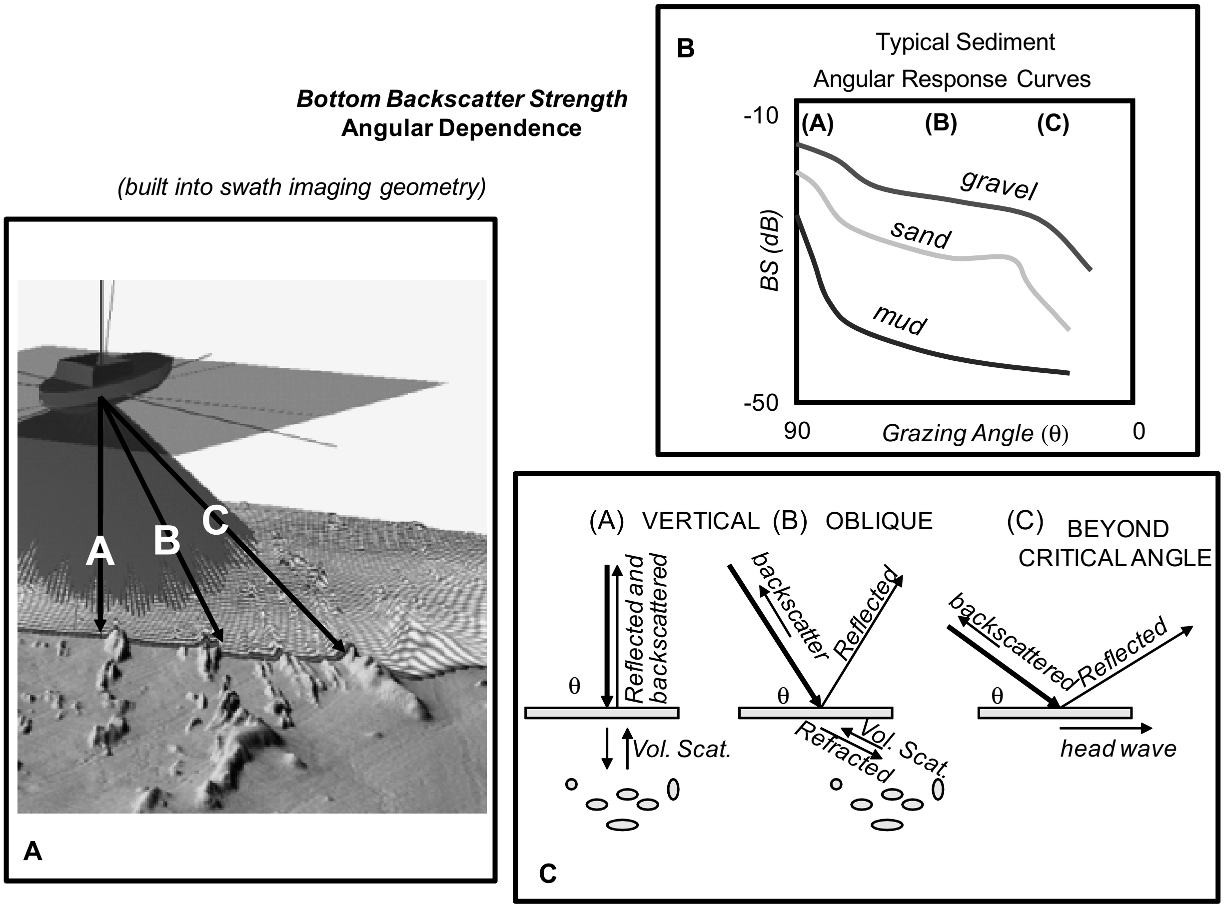

Fig. 8. The effect of grazing angle on multibeam geometry and typical angular response curves. Cartoons illustrating the changing role of the differing physical scattering processes for the three main parts of the angular response curve are shown (Vol. Scat. = Volume Scattering, Critical = angle beyond which no sound is refracted into the seabed).

quantity such as grain size has been inferred (e.g. Borgeld *et al.*, 1999) but in general remains elusive because spatial variations in backscatter may reflect changes in one or all of the following:

- Impedance contrast of the seabed/seawater interface (controlled by the bulk density and sound speed in the sediment);
- Interfacial roughness of that sediment water boundary;
- Volume heterogeneity – changes in the patchiness and contrast in the very shallow subsurface impedance;
- Changing grazing angle (Fig. 8).

Even at a fixed grazing angle, it can thus be ambiguous as to whether a change viewed is resulting from a change in impedance, roughness, or volume heterogeneity. Hamilton & Bachman (1982) demonstrated that, for terrigenous sediments, the impedance is strongly correlated with grain size. It would be convenient if this were the principal control on backscatter strength but, for a given grain size, the interface roughness is linked to other factors such as sorting or rippling or the presence of shell hash. For fine-grained sediment (where there is significant penetration into the sediment), the volume heterogeneity is controlled strongly by bioturbation and/or the presence or absence of buried shell debris or glacial dropstones.

Distinguishing outcrop or cobbles from fine-grained unconsolidated sediments is not an issue as the backscatter strength contrast between gravel and mud is unambiguous for all grazing angles (Fig. 8B). For the case of most temperate continental shelves, however, the variations of interest often range only from muddy sands to sandy muds. Under these conditions, the simple grain-size correlation can be obscured by other factors such as sorting, rippling, bioclastic debris and bioturbation.

Grazing angle effects

Even for a given set of sediment physical properties, the backscatter strength will vary with grazing angle (Fig. 8B). A typical swath will image from vertical incidence (90° grazing) to grazing angles usually as low as 25° (Fig. 8A). Thus, a measure of bottom backscatter strength will vary across the swath, providing at first glance, a misleading picture of the sediment distribution. For practical mapping purposes, the geological interpreter wishes to view an image that reflects regional sediment variations without having to continuously be aware of the imaging geometry. To achieve that, a compensation algorithm needs to be established that effectively "flattens" the angular response curves (Fig. 8B). To do this, of course, requires *a priori* knowledge of the shape of that curve.

The curve shape however, is highly variable between differing sediment types with strong specular peaks, of varying width and differing rates of roll-off with low grazing angle (Fig. 8B). Thus there is a need to locally adjust the compensation algorithm to reflect the local angular response (AR) curve. However, this is potentially a circular argument, as the AR curve needs to be derived from the seafloor and thus one needs to assume that the sediment type is constant from side to side in a single (or series of adjacent) swath. For continental shelf depths (50–200 m) this translates into an assumption of spatial sediment invariance over a distance of 200 to 800 m. Without this assumption one risks interpreting across track sediment changes as unusual AR curves which could then be compensated incorrectly.

Sonar radiometric and geometric influence on the received scattering intensity

All of the above discussion assumes that one has a calibrated measure of the bottom backscatter strength (BS). To achieve this requires a complete knowledge of the sonar system settings.

Source level and receiver gain settings

Depending on the sonar system, the source level and receiver gains may or may not have already been compensated for. For Kongsberg systems, the receiver gains are automatically set to adjust for source level, spherical spreading, attenuation and pulse length and seabed backscatter variations (but assuming a locally flat seafloor) (Hammerstad, 2000). The only compensation necessary for these systems is slight adjustments for exact pulse length used, beam pattern residuals (see later section) and true seafloor slope (see later section). In contrast, the RESON family of sonars maintain a fixed receiver gain ramp but log all the radiometric parameters including source level, pulse length and fixed gain steps. Before data can be used for geological interpretation, all the calculations need to be applied in post processing (e.g. Beaudoin *et al.*, 2002).

The most fundamental measure is the source level of the sonar. Few multibeam systems are precisely calibrated and thus an absolute level cannot be relied upon. The usual proxy is that, for the duration of a deployment, the source level is a constant. Such an assumption will break down if a survey consists of multiple deployments with changing sonar hardware. Overlapping coverage between surveys performed with different hardware settings may be the only way to maintain a stable relative calibration (Hughes Clarke *et al.*, 2008). Thus when trying to quantitatively assess whether a change in backscatter imagery between two surveys is real, the user must attempt to grossly shift the data to match in regions where it is believed that the seabed sedimentary environment is unaffected. Even if the data in a certain region are fixed, one needs to account for the effect of changing seasonal oceanography, which is expressed in the seawater attenuation coefficient.

Seawater attenuation

The received intensity is a function of the attenuation taking place in the seawater. This attenuation is dependent on the frequency of choice and varies significantly with temperature and salinity (Francois & Garrison, 1982a, b). It is up to the user to apply the appropriate value. One of the main variations reflects the changes in fresh water influence as one moves within the coastal zone. For example at given salinities the received intensity (all at 10 m depth, 10 °C, 100 kHz):

- 33 ppt salinity (typical coastal ocean): 32 dB km^{-1};
- 27 ppt salinity (typical distal river plume or fjord basin): 27 dB km^{-1};

- 15 ppt salinity (typical brackish estuary): 16 dB km^{-1}.

Fortunately river plumes are normally restricted to the upper few metres of the water column and thus the depth-averaged attenuation coefficient is less affected. But within fjord basins, separated by sills, the bulk change in the salinity from basin to basin, if not accounted for, will alter the apparent backscatter strength of the basin floor. For example in 100 m water depth using a 60° beam (400 m round trip) this corresponds to a 2 dB change for a change from 27 to 33 ppt. Thus, unless compensated for (not standard in most post-processing software), one cannot discern whether there is a change in the sediment type up the fjord, or merely a change in the water mass.

Perhaps more misleading is the fact that such a bias is depth dependent. For a single basin, the image will appear consistent, but, with the wrong attenuation coefficient, the interpreter may infer a depth-correlated change in sediment type. Using the same example (33 v. 27 ppt), the same material will appear 4 dB weaker from the beach to 200 m depth and 8 dB weaker at 400 m depth. Compared with that, the BS variation between fine sand and mud is only 2–6 dB. Many sedimentary environments are depth-dependent as they depend on surface wave activity or current strength and thus the user is easily led into believing depth-related apparent sediment variations.

Another effect is the seasonality of the water temperature (all at 10 m depth, 33 ppt S – 100 kHz):

- 5 °C – 27 dB km^{-1};
- 10 °C – 32 dB km^{-1};
- 15 °C – 35 dB km^{-1}.

Thus if a regional survey starts in the spring (5 °C), but continues, or is compared with one in the late summer (15 °C), a 100 m depth solution using a 60° beam, (a 400 m round trip) will exhibit a 3.2 dB difference.

Pulse length changes

Except when operating in the shallowest range of depth, most sonar systems are operating at full power the upper level of which is normally restricted by cavitation issues. As the water gets deeper, the received signal strength will drop, resulting in a loss of signal to noise. To circumvent this, one needs to increase the pulse length. Doing so for the same source level increases the instantaneously ensonified area resulting in both a stronger signal and, for narrow band signals, a lower range resolution.

This has three effects on the geological interpretation:

1. Unless compensated for, the seabed intensity will appear to change. Even for those systems that do so, the compensation is never perfect;
2. If the interpreter is relying on the pixel speckle characteristics to discern different sediment type, the speckle pattern will coarsen with longer pulses;
3. If the interpreter is looking to resolve small features, the longer pulse will be defocused, making some short wavelength features such as ripples or cobble fields disappear.

To compensate for effect 1, a measure of the pulse-length needs to be maintained with the data and, based on analysis of the shift at changes, a bulk and/or range and angle-dependent offset needs to be applied.

The second effect can be most damaging to some of the automated textural classification software on the market (e.g. Milvang *et al.*, 1993; Preston *et al.*, 2001) both of which in part rely on the "Pace" features (Pace & Dyer, 1979; Pace & Gao, 1988). At this time, this approach cannot take into account pulse length changes and thus automated classification is limited to regions where a single pulse length is used.

For the third effect, the loss in resolution is generally less of an issue because, at the point at which the pulse length needs to be shifted, the data with the shorter pulse length are compromised in any case by the lower signal to noise levels.

Beam patterns – single and multiple sectors

Both the transmitter and each of the individual receiver beam patterns have intensity/sensitivity variations with elevation angle. The combined effect of these two beam patterns will generate variations in received intensity across the swath that might be confused with seabed sediment changes.

The simplest configuration is a single-headed, single sector, multibeam in which the entire swath is illuminated by one transmitter. In this case, the transmit beam patterns are generally simple, varying only slowly with angle (e.g. RESON 8111, Beaudoin *et al.*, 2002). A notable exception is the original EM1000 which used a barrel array for the transmit and thus variations in the intensity from the staves within the barrel could produce complex transmit beam patterns. In both cases, the pattern is fixed with respect to the array. For the EM1000, because each receiver channel, which is roll-stabilized, uses a separate amplifier, any inter-amplifier differences will show up as an apparent vertically-referenced beam pattern residual.

An additional complication is found in multi sector systems. Several systems: EM12, EM1002, EM300, EM120, EM710 use multiple sectors. This is done to provide advantages in multiple suppression, improved pitch and yaw stabilization (Fig. 3), improved water column imaging (Hughes Clarke, 2006) and to allow transmit focusing (Kongsberg, 2005). Each sector has a unique center frequency to avoid interference between sectors. As a result each sector may have slightly different calibrations. Also the seabed angular response can be subtly different at the different frequencies and each frequency has a slightly different attenuation coefficient. All these factors conspire to make the sector boundaries show up in the backscatter data (Llewellyn, 2005), potentially confusing geological interpretation.

In the worst case, both sonar-referenced and vertically-referenced beam pattern artefacts may be apparent in the data and require compensation. Figure 9 is an example of this, although using data from a malfunctioning sonar to better illustrate the effect. The data are from an EM1002 that has three transmit sectors whose beam patterns are fixed with respect to the sonar. The same sonar receivers are roll stabilized and thus vertically referenced. Thus one sees the effect of rolling transmit beam patterns truncated at the vertically-referenced sector boundaries. An estimate of the beam pattern (described below) has to be collected separately for each of the sectors. Once estimated, by combining this with knowledge of the vessel roll at transmit, the two signatures may be predicted and removed from the data. As stated, this is an extreme example with > 10 dB beam pattern nulls. However, such signatures at levels of only 2 dB are still common and hamper interpretation of typical continental shelf seabed sediment signatures that are of similar magnitude (Iwanowska *et al.*, 2005). More typically, only the vertically referenced sector boundaries show up (Figs. 10 and 11).

Backscatter data manipulation strategies

Given all the imperfections outlined above, the real-time backscatter output of the multibeam sonar systems will contain artefacts that hamper the ability to undertake regional sediment distribution analysis (e.g. Fig. 11A). The most noticeable effect is that of residual beam pattern and grazing angle distribution. Thus strategies need to be developed to minimize these artefacts.

Estimating residual beam pattern and grazing angle variability

In order to remove the beam pattern and grazing angle effects, one ideally needs to know the transmit and receive beam pattern sensitivities (by sonar and/or vertically referenced angle, Fig. 9) as well as the local seabed angular response curve (by seafloor grazing angle, Fig. 8). As these are all unknowns, this must be guessed based on the intensity variations by a combination of sonar-relative, vertically-referenced and seafloor-referenced angle. Unless one of the three signatures is dominant, it is practically impossible to separate them. Thus the vertically referenced angle is usually used, as, averaged over several 100 or 1000 pings, the sonar-relative angles will oscillate about zero and the seafloor slope will on average be level.

The operator is left with a choice of length scale over which to average. The longer the averaging, the more likely that local across-track geological variations will average out. An array of intensities by beam referenced angle is maintained (e.g. Fig. 9A) and the statistics of the average intensity, normally in 1° bins, is compiled. A reference level representative of the average signal strength is then selected and intensity offsets (multipliers in linear intensity or additive offsets in logarithmic intensity) are calculated for each 1° bin. The data are then adjusted so that all beams at a certain 1° bin have a fixed offset in intensity applied.

Coping with geographically varying angular response curve shapes

Given the strong beam pattern and grazing angle signatures that will be present in multibeam backscatter data, strategies need to be established to minimize these. Figure 10 illustrates strategies for achieving this.

For a single line, statistics can be gathered on intensity variations with incidence angle. Averaged over many geological terrains (as would be covered in a typical survey line), this represents the best guess of the combined input of beam pattern and grazing angular response.

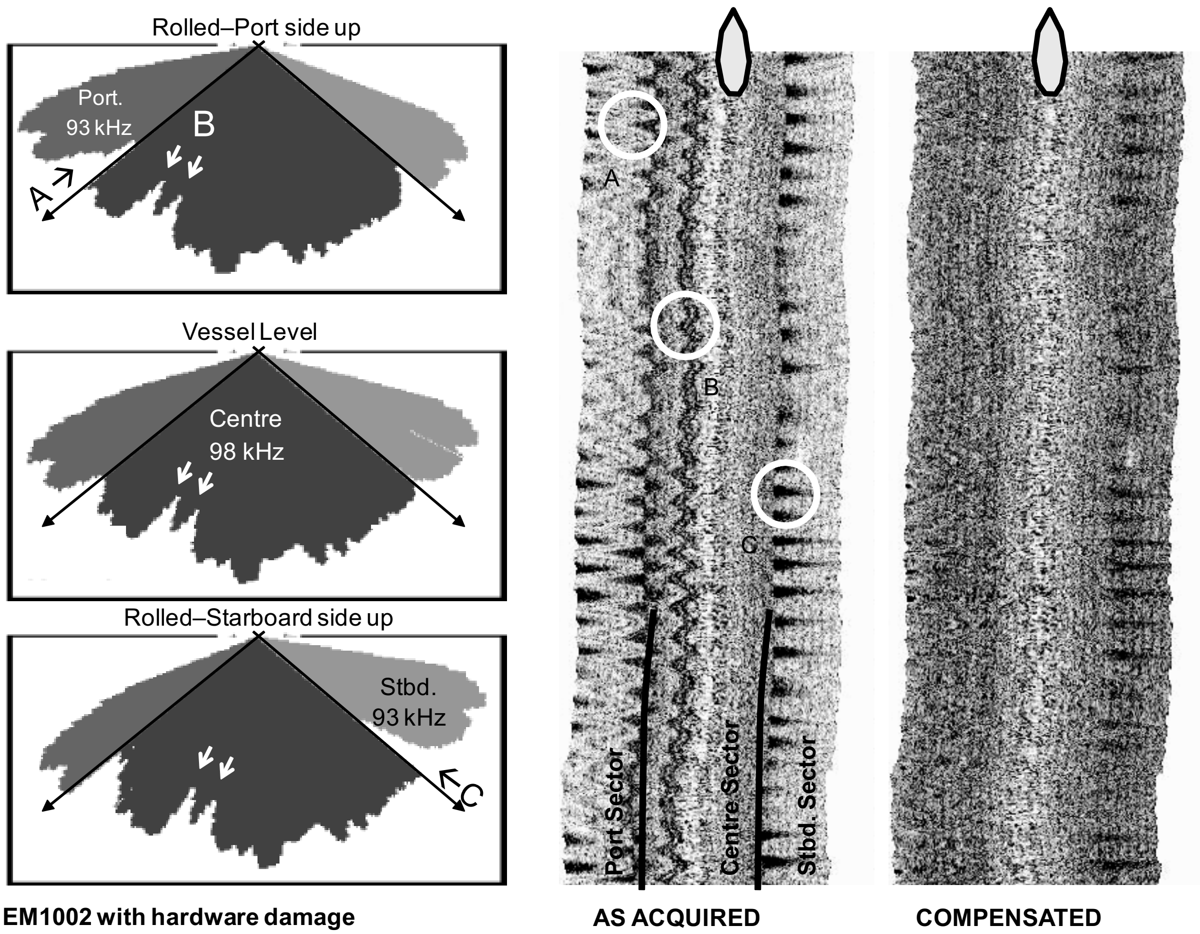

Fig. 9. Special case processing for multi-sector multibeam backscatter data. The example presented (data courtesy of the Geological Survey of Israel) has a hardware problem resulting in pronounced transmit beam pattern residuals (shown by A, B and C). Statistics are compiled separately for each sector. The sector data are collected within specific vertically referenced sectors, but compiled by sonar-relative angle. While this is an extreme example for illustrative purposes, such patterns impede geological interpretation and should be removed.

The main limiting assumption is that the shape of the AR curve for all sediment types, while of different mean level, is the same shape. However, the shape of the AR curve for different shelf sediments is highly variable (Fig. 8B), some having strong and narrower specular peaks, others have differing roll-off with low grazing angle, sometimes including a critical angle cusp.

Thus it would be better to calculate this combined response separately for each sediment type. This requires, however, an *a priori* knowledge of the sediment distribution. One way to approach this is to derive the statistics not regionally (i.e. the whole line, or several lines) but locally (for a subset of the line). However, the danger comes when one tries to define what locally is. If sediment type changes over length scales of hundreds or thousands of pings, one can select a similar length scale, but for such a small number of pings, one may remove the valid assumption of geological randomness. This is easiest to visualize by thinking of sediment being different from one side of the swath to the other for the duration of the averaging period. An apparent lop-sided angular response estimate will result and the correction will attempt to flatten it.

Figure 10 illustrates this dilemma. Image (A) shows the EM1002 data with the Kongsberg flattening function applied. While the gross sediment boundaries are visible, the sector boundary is overprinted and it is clear that the near-nadir backscatter data is imperfectly flattened. Figure 10B shows the result of estimating the response over the entire line. The sector boundaries are now

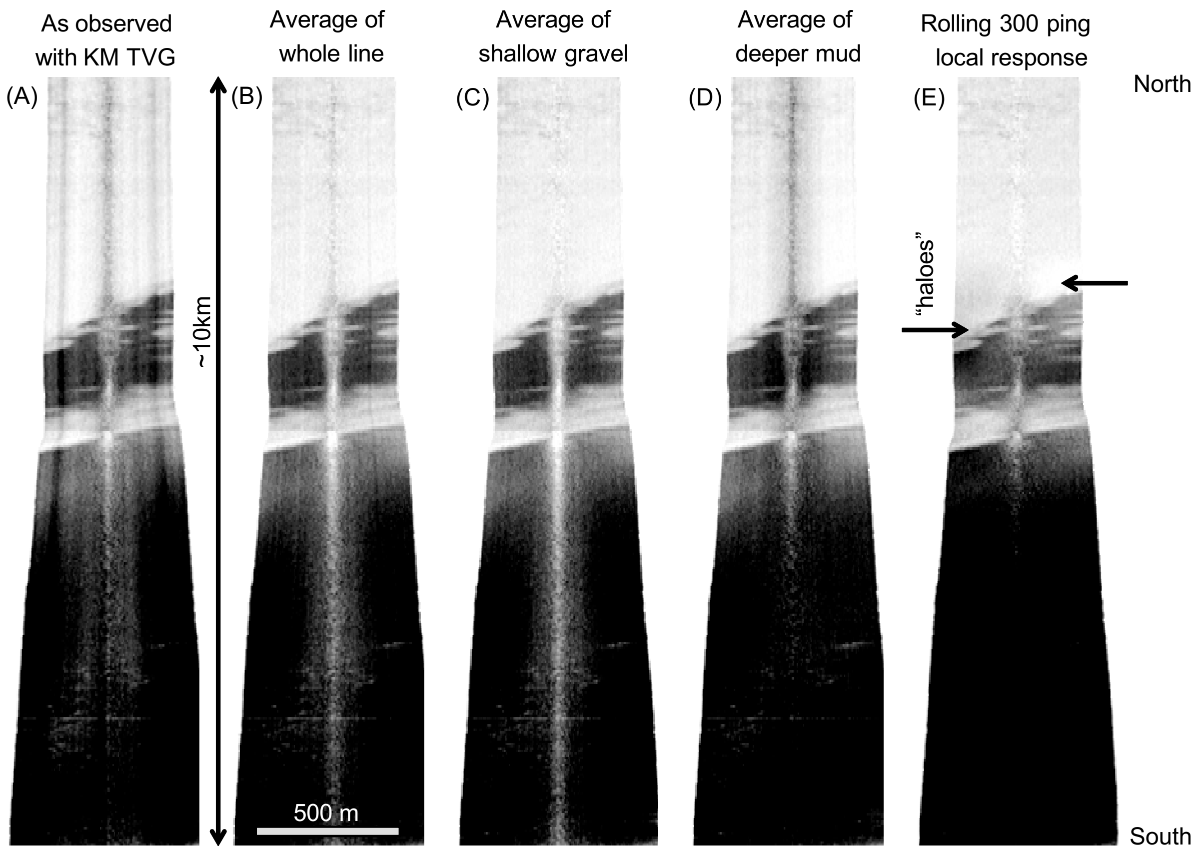

Fig. 10. Empirical approaches to predicting and removing combined angular response and transmit-receive beam pattern products. Data are a 10 km line collected with a $\pm$ 65° sector, running from $\sim$ 100 m depth gravels in the north to $\sim$200 m deep muds in the south. (A) Beam trace data as delivered by Kongsberg Maritime (KM) using their predictive time varying gain (TVG) functions. Note the presence of pronounced beam pattern residuals at the sector boundary transitions at $\pm$ 50°. (B) Data after application of corrector for line-based (all 4600 pings) average intensity by vertically referenced angle. Note the removal of the sector boundary artifacts, but over compensation of the nadir response in the northern gravels and under compensation of the nadir response in the southern muds. (C) Data after application of corrector based only on northern gravels (first 2000 pings). Note good compensation for gravels, but under compensation for muds. (D) Data after application of corrector based only on the southern deep muds (last 2000 pings). Note the good compensation for the muds, but over compensation for the gravels. (E) Data after application of a rolling 300-ping-based local corrector. Note the excellent suppression of the nadir response throughout the whole line. One caveat is the "halo" effect on traversing abrupt oblique sediment boundaries.

subdued (as they were present for the whole line) but it is apparent that the near nadir response is under compensated at the north end of the line and overcompensated at the south end of the line. Figure 10C and D illustrate the effect of using statistics from just the northern or southern end of the line. In each case, the flattening algorithm is superior in the region from which the statistics are derived but fails on the other sediment type.

The important factor here is the contrast between the flat near-nadir AR of gravels and the peaked near-nadir and steep low grazing angle drop off typical of muds (Fig. 8B). In Fig. 10E a strategy of continuously estimating the local incidence angle–referenced response over a length scale of 300 pings was employed. As can be seen, this approach best regionally suppresses the angular response. What is less apparent, however, is that this method produces artefacts at sediment boundaries where the sediment is not uniform from one side of the swath to the other ("haloes" in Fig. 10E).

Figure 11 illustrates the approaches described above for a large continental shelf region (Hecate Strait, Barrie, 2004, pers. comm.). Figure 11A is the original data, while Fig. 11B shows the line-based strategy and Fig. 11C the rolling response strategy. A general improvement in the clarity of the likely sediment distribution is apparent. Two

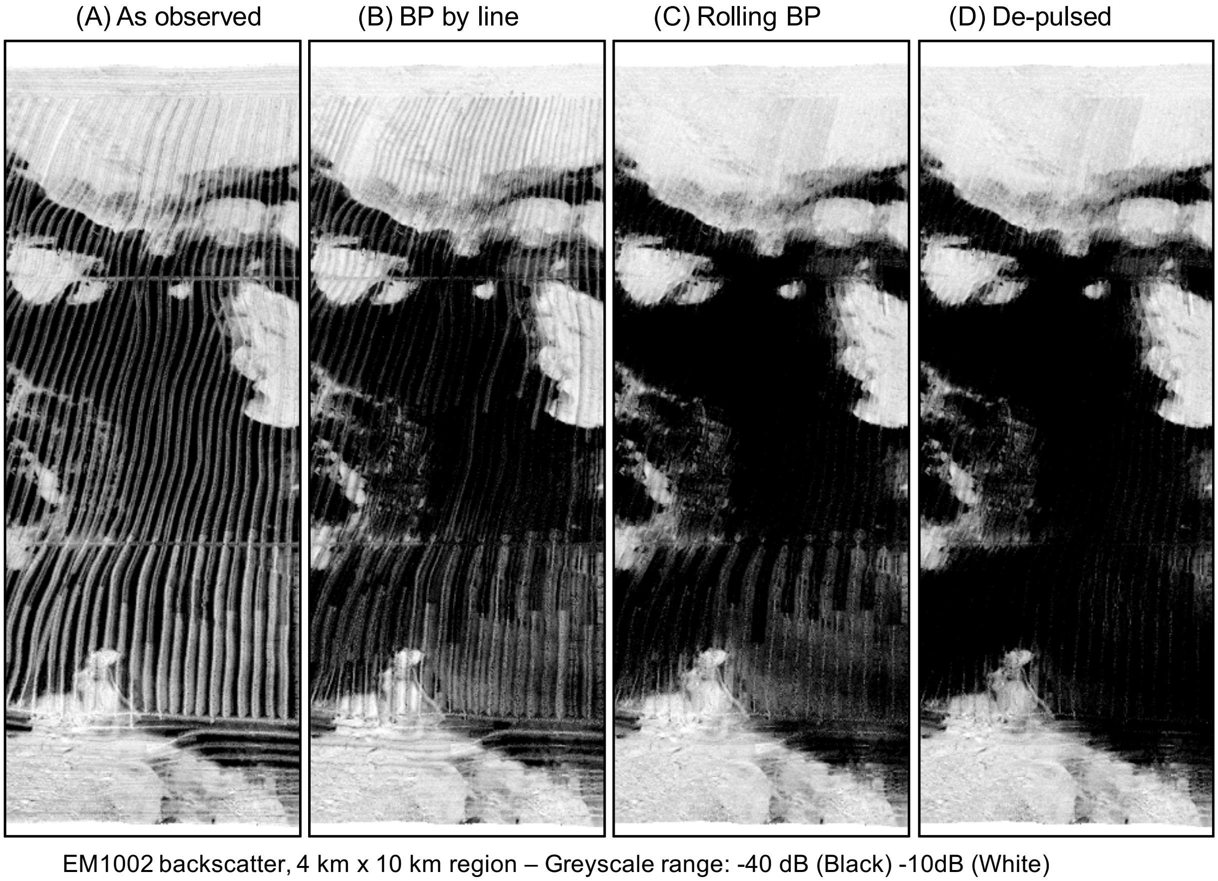

Fig. 11. Successive processing steps for EM1002 backscatter data. Data were collected in ~ 150–250 m of water using a $\pm 65°$ sector. In the southern half of the survey, the depths were great enough to cause the sonar to jump from a 0.2 ms pulse to a 0.7 ms pulse. (A) Original data with just Kongsberg 1st order TVG reduction. (B) Data empirically processed on a line-by-line basis, reducing for the effects of average across track intensity by vertically referenced grazing angle (BP = beam pattern). (C) Data empirically processed with a rolling 500 ping local incidence angle function. (D) As in C but with an empirically calculated offset for the 0.7 ms pulse data (-2 dB). Note that even after this it is apparent that, half way across the survey, there is a jump in backscatter (of only $\sim$2 dB) due to in-field replacement of the transceiver electronics board.

final artefacts are still apparent, however. The pulse length was increased for the lines in the southern end of the area. In Fig. 11D an empirical correction was applied to account for this. Even after that, however, it is apparent that there is an abrupt small, but noticeable, gain offset half way across the image. This was due to replacement of sonar hardware on board, mid way through the cruise. Thus, even after all these steps, it would be hard to be confident in a regional change in seabed sediment type based on a resurvey.

While at first it may appear that the rolling response predictor (Fig. 10E and Fig. 11C) is the optimal approach for interpretation of continental shelf sediments, it is actually hiding valuable information from the interpreter. The grazing angle response of the sediment has been specifically removed so that a particular sediment type will appear at the same grey level irrespective of ensonification angle. However, there are many shelf sediment types that exhibit very similar AR curves and that may be identical in the mid-grazing angle range, but differ near nadir or at low-grazing angles. Figure 12 illustrates this concept. Image (A) is as collected. Image (B) is after rolling response correction. The second image is more pleasing to the eye, but between the two areas circled in (A), there is actually a change in sediment type. The two AR curves (Fig. 12C) are identical in the mid range of grazing angles but one has a stronger specular peak than the other. They are probably similar sediments with similar volume scattering signatures (that dominate the mid-range of grazing angles) but one has a smoother interface than the

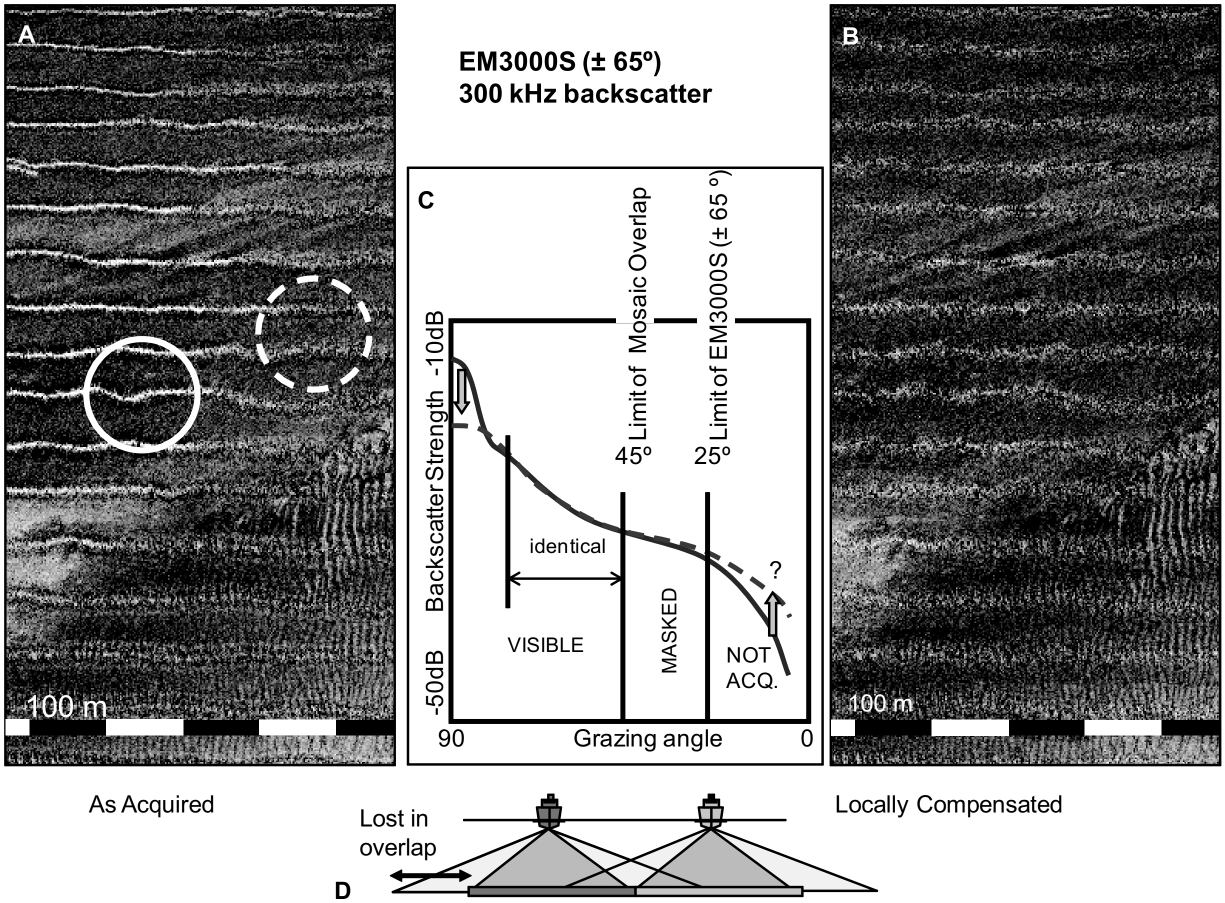

Fig. 12. Effect of using the rolling empirical combined beam pattern and grazing angle corrector. (A) is original data; (B) is after use of corrector. Note the improved cosmetic appearance of the image. Characteristic aspects of the angular response curve (C) have been lost, however, that would allow improved discrimination of sediment types that appear otherwise of similar mean backscatter strength. Further information available at the lowest grazing angles is not in the overlap strategy used in typical mosaicing (D).

other. This extra degree of freedom in discrimination has been lost to the operator.

Additionally, in Fig. 12D one can see that the mosaicing method has suppressed the low-grazing angle data as the survey has significant overlap. These two sediment types actually have different low grazing angle responses but this is obscured from the interpreter. Methods that classify and present the shape of the angular response curve such as Hughes Clarke (1994) or Hughes Clarke *et al.* (1997) are needed to improve discrimination.

Local grazing angle extraction

The above described backscatter data reduction recognizes that two systematic signatures exist in typical multibeam data: firstly, the sonar transmit and receive radiometric signature which may be either (or both) referenced to the vertical or sonar-relative reference frame (e.g. Fig. 9) and secondly, the seabed itself provides an angular signature that is, in contrast, referenced to the local seabed surface normal. The majority of unconsolidated continental shelf sediments rarely exhibit seafloor slopes over a few degrees, and thus to a first order, the grazing angle signature can be approximated as a vertically-referenced signal and therefore treated simultaneously with the radiometric issues.

If, however, there are gross changes in slope, or more noticeably, if there is a particularly steep grazing angle response (e.g. close to normal incidence), the difference between the grazing and incidence angle can become important and confuse geological interpretation.

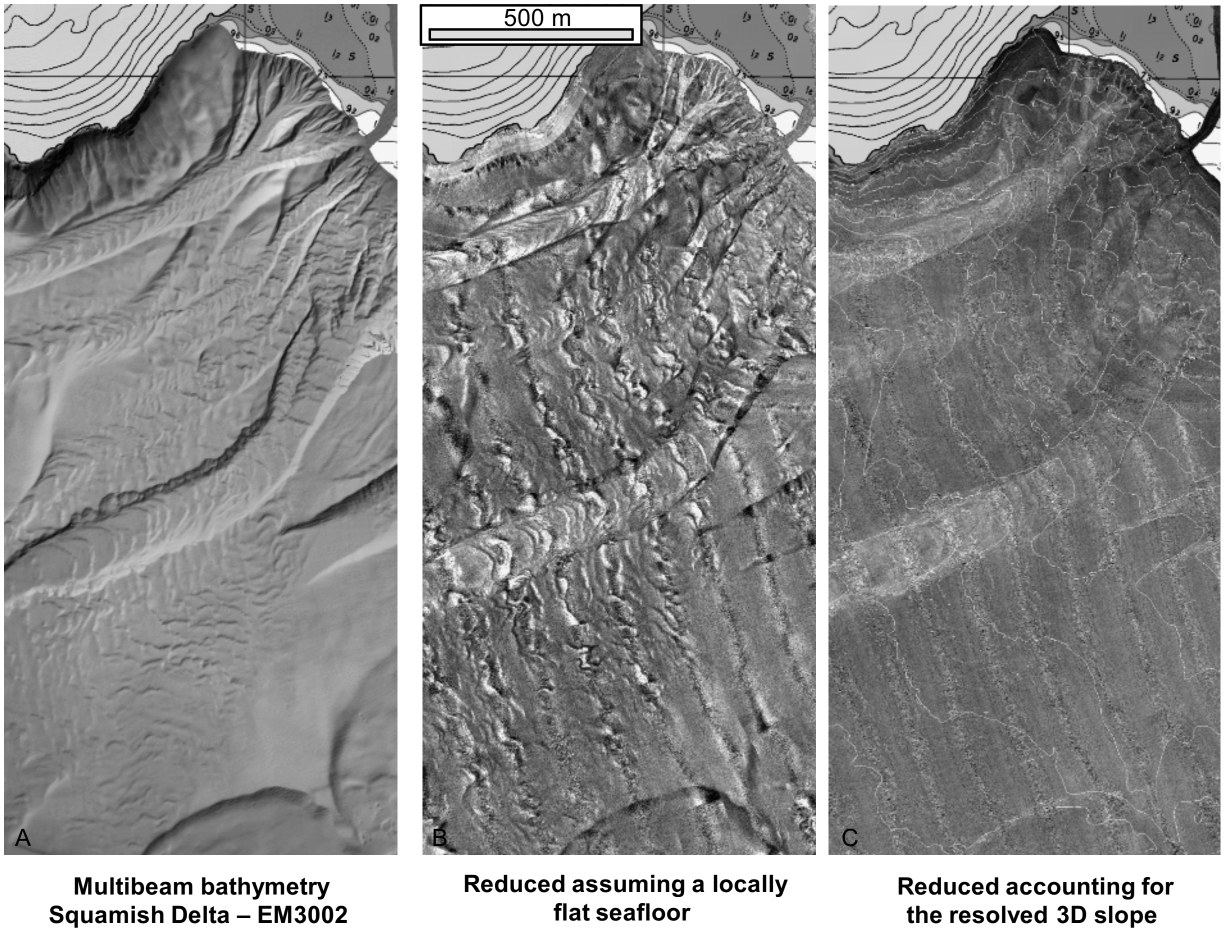

Fig. 13. (A) Sun-illuminated bathymetric image of the Squamish Delta upper delta face. (B) Standard output 300 kHz backscatter map products assuming locally flat seafloor. Note that there appear to be significant seabed backscatter strength fluctuations that correlate with the bedforms developed on the foreslope. (C) Modified image accounting for seabed-relative grazing angle. After correction one notes that the relief-correlated apparent backscatter strength modulations are gone. These modulations were thus driven by grazing angle and not variations in seabed type. Grab sample analysis confirms that there are no significant fluctuations on the sediment type over the bedform fields.

For example, one of the major ambiguities is determining whether a signature in the backscatter is due to textural (i.e. sediment type) variations associated with changes in slope, or simply the changes in slope itself. This dilemma is most apparent for the case of bedforms. Most bedforms exhibit a change in sediment type from stoss to trough and thus a banded backscatter signature is to be expected.

Figure 13 illustrates the removal of the grazing angle signature from a survey of bedforms on a delta front. The original logged backscatter data (Fig. 13B) exhibited a signature strongly correlated with the bedforms visible in the topography (Fig. 13A). In this case, there was assumed to be no significant beam pattern component and the response was compiled by seabed-reference grazing angle. After correction for this (Fig. 13C) it is apparent that there is no significant change in sediment type from stoss to trough of these bedforms.

DEMONSTRATION OF CHANGE DETECTION CAPABILITY AND LIMITATIONS

In order to illustrate together all of the components of the absolute accuracy and potential for change detection, an example pair of overlapping multibeam surveys are presented. The data illustrated (Figs. 14 and 15) cover a field of bedforms on the floor of the Bay of Fundy off Margaretsville, Nova Scotia. The bedforms lie in 50–70 m of water in a region where the tidal range is ~9 m and peak tidal currents of over 2 knots are present in the area running roughly in a linear trend 050T-230T.

The data were collected at two times with two quite different sonar configurations (those presented in Fig. 2):

- 1994 – a Simrad EM1000 was used on board the CCGS Frederick G. Creed. The EM1000 operates with a single frequency sector at 95 kHz. The sector is roll stabilized only. The system operates with beam width of 2.4° in transmit and 3.3° in receive. Because the EM1000 is a barrel array, the 3.3° receive beam is maintained to 60° off vertical only opening to 3.4° at 75°. For these operations, 60 beams were used in an equi-angular spacing over a 150° sector. The pulse length used was 0.2 ms and typical repetition rates were ~ 2 Hz. The vessel was operating at 14 knots (resulting in typically 3.5 m along-track beam spacing) running lines with only ~10 % overlap in a NE-SW direction. The EM1000 was integrated with a TSS-335B motion sensor which was only rated to 0.25° and was sensitive to cornering. The positioning used was a local differential base station, 80 km way and intermittent loss of correction was experienced. On average, total horizontal positioning accuracy is estimated to be about 5 m. The data have been reduced using the WebTide model.
- 2007 – a Kongsberg EM710 was used on board the CCGS Matthew. The EM710 operates using 3 sectors: 97 kHz in the central (± 40°) sector, 83 kHz in the starboard sector and 71 kHz in the port sector. The three sectors are roll, pitch and yaw stabilized. The system operated with a 0.5° transmit beam width and a 1.0° (at broadside) receive beam width. Because it is a flat line array, steered receive beams grow with obliquity, for example the receiver beam at 60° is 2° wide. 256 physical beams are formed in an equi-angular manner over a 130° sector. Within the outer beams, multiple bottom detections are generated (termed high-definition beam forming), resulting in an equi-distant spacing of 400 sounding solutions over the swath spaced on average at about 50 cm. The pulse length used was 0.16 m and typical repetition rates were 4 Hz. The vessel was operating at 10 knots resulting in typically 1.25 m along-track spacing.The EM710 was integrated with a POS/MV 320 v.4 which is rated to 0.02° and is insensitive to high speed cornering. The positioning system used was Fugro OmniSTAR HP (Visser, 2007) with a predicted horizontal accuracy of ~ 20 cm. While the vertical component of OmniSTAR is being investigated as a source of vertical control, for this demonstration the WebTide model is used for vertical referencing in the identical manner to the 1994 data.

For both surveys, sound speed profiles were obtained at about 6-hourly intervals. However the extent of mixing in this macrotidal area in the inner Bay resulted in there being little spatial variability in the sound speed field.

In Fig. 14 we can compare the two bathymetric images. The regional data are presented as a 5 m grid, which fails to capture the full resolution of the EM710. The zoomed image to the left is regridded at 2 m for the EM710 to demonstrate that it is capturing 4 m wavelength dunes in 65 m of water. Even at the 5 m grid size, however, the limit of the EM1000 bathymetric resolution is apparent (Fig. 14A left).

A difference map is presented (Fig. 14C) illustrating the apparent surface difference in the region. Corridors of apparent change are visible over scales of a swath width, resulting in linear steps in the difference maps that align with both of the survey orientations. This is a result of two factors. Firstly the WebTide model is failing to capture the true tidal signature in the area to better than about ± 40 cm, and secondly, especially for the EM1000 with its wider sector, refraction of the outermost beams shows up as outer beam negative ridges. The most noticeable step in the surface difference occurs when the EM1000 survey was broken off and only resumed after a day at a different phase of the tide.

Because of the tidal and sound speed imperfections, no confidence may be placed in any regional accretion or deflation of the seabed. Because however, dune migration in excess of the worst positioning accuracy (5 m for 1994) is apparent, one can assess the direction and scale of bedform migration in the area. The area is dominated by flat regions punctuated by at least three scales of bedforms. Solitary “whaleback” dunes of 5–15 m amplitude and 200–500 m length, transverse asymmetric dunes 1–2 m high and 40–100 m wavelength and dunes of wavelength of less than 10 m are resolvable with the EM710. The sense of migration (arrows in Fig. 14) of the solitary bedforms can be easily discerned and notably do not move in a

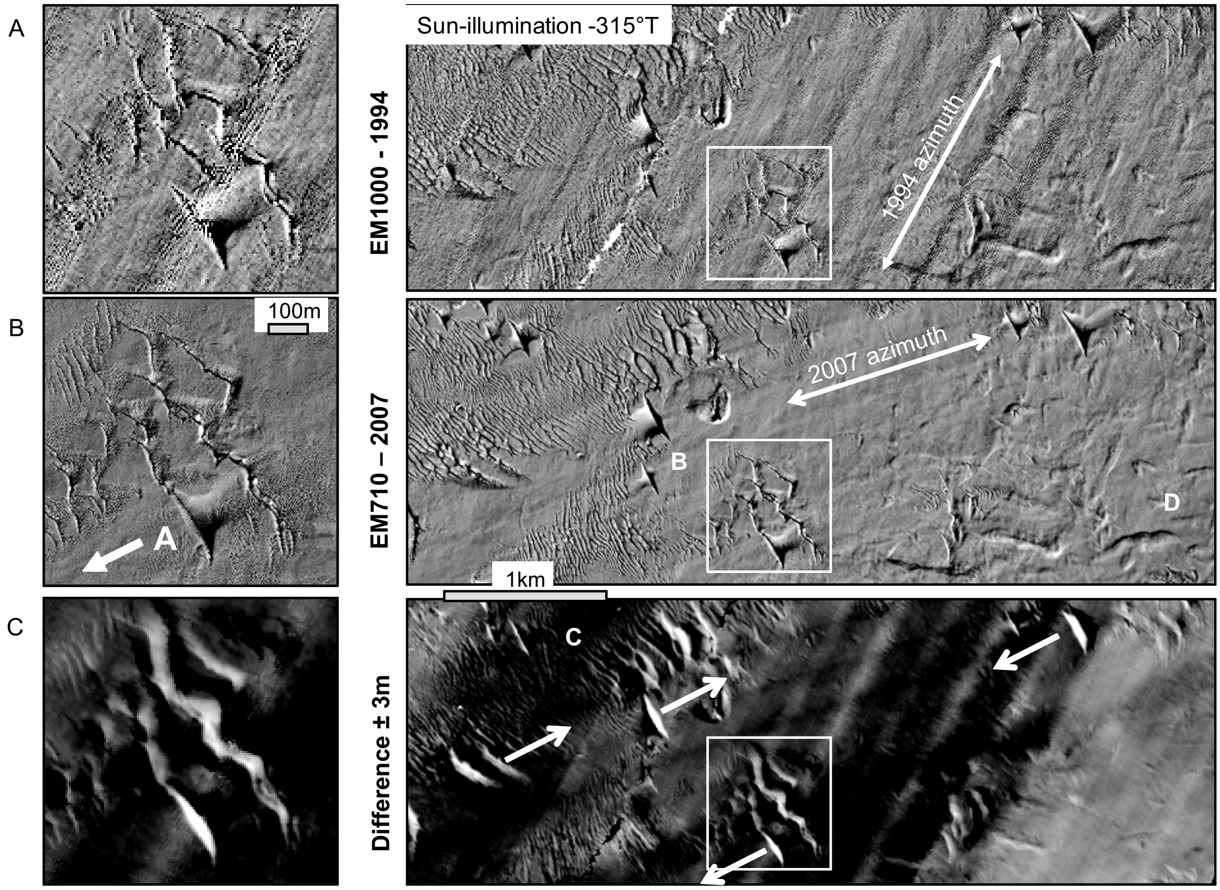

Fig. 14. Bathymetric comparison between two multibeam surveys. (A) 1994 EM1000 (95 kHz) 150° sector 10% overlap, Tx. 2.4°, Rc 3.3°. (B) 2007 EM710 (70–100 kHz) 130° sector, 100% overlap, Tx 0.5°, Rc 1.0°. (C) Difference map, 2007–1994 (greyscale –black −3 m, white +3 m). White boxes – zoom in of detail of 3 scales of bedforms. The arrows denote the directions of dune migration.

consistent direction. One can clearly see that the preferred migration direction is always away from the build up of a tail of sediment on one side (Fig. 14B, A and B migrating in opposite directions). The difference map clearly indicates that the intermediate wavelength dunes are mobile (C in Fig. 14C), but the direction and scale of migration direction cannot be discerned as the bedforms have clearly moved more than a fractional wavelength over the period (13 years), resulting in a loss of "lock". The scale of migration can be sensed by the fact that the boundaries of the dune fields have often shifted by hundreds of metres. There are also large regions in which no bedforms are apparent in the bathymetry, but a presumed relict glacial morphology is visible (D in Fig. 14B) as minimal bathymetric change is resolvable there.

Next the backscatter data changes are examined (Fig. 15). In both cases the data have been reduced for source level, pulse length, spherical spreading and attenuation by the manufacturer. Additional processing steps, as described in text, include empirical assessment of combined beam pattern and average seabed angular response. In order to match the two surveys, a bulk shift of 6 dB was necessary indicating a lack of confidence in absolute calibration of one or perhaps either sonar. As the depth ranges were small, attenuation coefficient choice was less important.

When differencing the two backscatter images, one has to be careful of changes in grazing angle. The empirical grazing angle suppression algorithm has minimized this so that the dominant signature is not along track differences that follow grazing angle. Along with the migration of the solitary bedforms apparent from bathymetric differencing, one can see a similar displacement in the backscatter differencing.

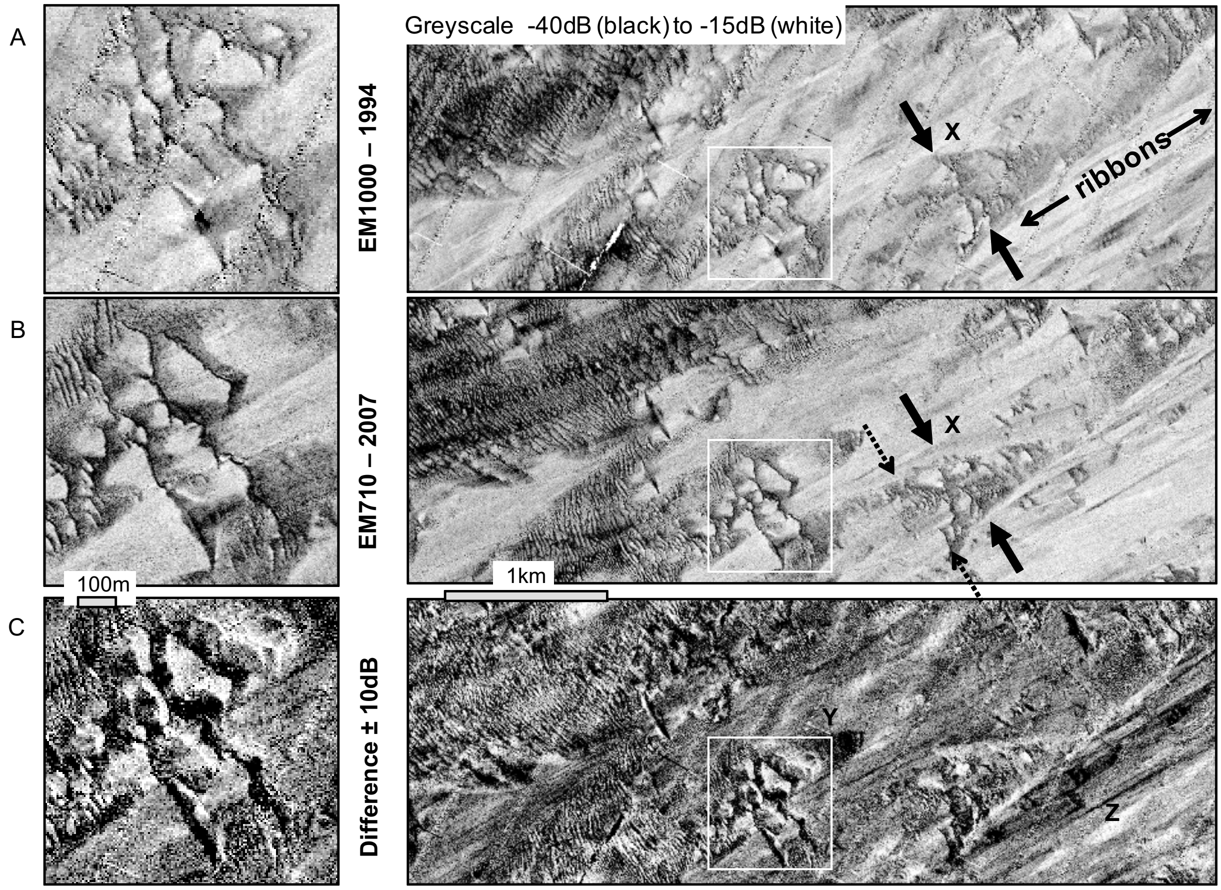

Fig. 15. Backscatter comparison between the same two surveys as Fig. 14. (A) 1994. (B) 2007. (C) Difference. Backscatter greyscale range: white −15 dB, black −40 dB. For an explanation of arrows and letters used in the figure, see text.

The backscatter provides information on both the individual bedforms as well as the regional substrate in which they are developed. The boundaries of the intermediate bedform fields can be better discerned in the backscatter, providing a method to discern the translation of entire bedform fields. For example a triangular-shaped wedge of sand waves (indicated by arrows and X) is seen to have migrated ~ 400 m over the gravel pavement in this period. Other fields have just appeared (Y in Fig. 15C). But most interestingly, in regions without bedforms and with relict glacial relief (eastern part of image) there is a clear ribbon-like pattern developed in the backscatter parallel to the current flow that bears no relationship to the relict glacial morphology. This is strongly modified over the 13-year period (Z in Fig. 15) indicating that it is a modern rather than relict sedimentary signature.

The combined analysis of both the bathymetric and backscatter change over the 13-year period allows us to separate the active sedimentary processes from the relict environments. All this is possible only due to a combination of system calibration, strategies for minimizing error sources and empirical data post-processing methods. In the future, studies of shelf morphodynamics will be increasing focused on this method of change detection and thus will require an increasing awareness of the error sources inherent in these systems.

CONCLUSIONS

Multibeam bathymetry and backscatter are providing an unprecedented view of co-located bottom morphology and surficial sediment distribution over continental shelf areas. While regional scale variations are easily discernable, to take full advantage of the resolving potential of the systems a series of artefacts are described and their proper manipulation discussed. Without proper understanding of the likelihood of these artefacts, interpretation of continental shelf morphodynamics could be hampered.

For continental shelf operations, the principal concerns for the bathymetric accuracy component are the tidal and water mass reduction. *A priori* knowledge of the propagation of the tidal wave across the region, and the typical distribution of watermasses in the area at the time of the survey, will represent a significant advantage in achieving repeatable bathymetric accuracy.

For the backscatter data processing, the principal concern is adequate reduction of the data for radiometric and geometric control on backscatter variability. Of these, the hardest two components are beam pattern residuals that result in incidence angle variation and seabed grazing angle dependence. For the first, in the absence of *a priori* knowledge of the transmission and reception sensitivities, systematic stacking of data over representative regions can give an adequate indication of the beam pattern residuals. Care needs to be taken to account for changes in the beam pattern associated with sector boundaries, changes in pulse length and sector width.

Overprinted on the incidence angle variations is the seabed grazing angle response. Because this is sediment-type dependent, extra care needs to be taken to estimate this locally and then compensate for it.

ACKNOWLEDGEMENTS

This research was funded through the sponsors of the Industrial Research Chair in Ocean Mapping at UNB. Current sponsors include: the US Geological Survey, Kongsberg Maritime, Royal (UK) Navy, Fugro Pelagos, Rijkswaterstaat and the Route Survey Office of the Canadian Navy.

EM1002 data from Hecate Strait were kindly provided by Vaughn Barrie and Kim Conway of the GSC-Pacific. EM1002 and EM3002 data from Squamish were provided by Phil Hill of GSC-Pacific and Kal Czotter of CHS-Pacific. EM710 data from the Bay of Fundy were provided by Russell Parrott of GSC-Atlantic and Mike Lamplugh of CHS-Atlantic.

REFERENCES

Admiralty (1969) Admiralty Manual of Hydrographic Surveying - Chapter 1 - Tides and Tidal Streams. In: *The Hydrographer of the Navy*, **2**, (Ed. G.S. Ritchie), Taunton, Somerset, N.P.134b (2).

Beaudoin, J., **Hughes Clarke, J.E.**, **van den Ameele, E.** and **Gardner, J.** (2002) Geometric and radiometric correction of multibeam backscatter derived from Reson 8101 systems. *Can. Hydrogr. Conf. Proc.* CDROM, 25 pp.

Beaudoin, J.D., **Hughes Clarke, J.E.** and **Bartlett, J.E.** (2004) Application of surface sound speed measurements in post-processing for multi-sector multibeam echosounders. *Int. Hydrogr. Rev.*, **5**, 17–32.

Borgeld, J.C., **Hughes Clarke, J.E.**, **Goff, J.A.**, **Mayer, L.A.** and **Curtis, J.A.** (1999) Acoustic backscatter of the 1995 flood deposit on the Eel shelf. *Mar. Geol.*, **154**, 197–210.

Brucker, S., **Hughes Clarke, J.E.**, **Beaudoin, J.**, **Lessels, C.**, **Czotter, K.**, **Loschiavo, R.**, **Iwanowska, K.** and **Hill, P.** (2007) Monitoring flood-related change in bathymetry and sediment distribution over the Squamish Delta, Howe Sound, British Columbia. *US Hydrogr. Conf. 2007*, CDROM, 16 pp.

Butman, B., **Twichell, D.C.**, **Rona, P.A.**, **Tucholke, B.E.**, **Middleton, T.J.** and **Robb, J.M.** (2006) Sea floor topography and backscatter intensity of the Hudson Canyon region offshore of New York and New Jersey. *US Geol. Surv. Open-File Rep.*, 2004–1441. 2 maps.

Cartwright, D. and **Hughes Clarke, J.E.** (2002) Multibeam surveys of the Frazer River Delta, coping with an extreme refraction environment. *Can. Hydrogr. Conf. Proc.* CDROM., 22 pp.

Chance, J., **Gravely, J.M.**, **Roscoe-Hudson, J.** and **Kleiner, A.** (2003) GPS for global tide measurements. *Hydro Internat.*, October 2003.

Conway, K.W., **Barrie, J.V.** and **Krautter, M.** (2004) Geomorphology of unique reefs on the western Canadian shelf: sponge reefs mapped by multibeam bathymetry. *Geo-Mar. Lett.*, **25**, 205–213.

deMoustier, C. (1993) Signal processing for swath bathymetry and concurrent seafloor acoustic imaging. In: *Acoustic Signal Processing for Ocean Exploration* (Eds J.M. Moura and I.G.M. Lourtie), pp. 329–354. D. Reidel, Amsterdam.

Department of Fisheries and Oceans (2005) WebTide Tidal Prediction Model. http://www.mar.dfo-mpo.gc.ca/science/ocean/coastal_hydrodynamics/WebTide/webtide.html

Duffy, G.P. and **Hughes Clarke, J.E.** (2005) Application of spatial cross-correlation to detection of migration of submarine sand dunes, Special Publication on Marine and River Dune Dynamics, *J. Geophys. Res.*, 110, F04S12, doi:10.1029/2004JF000192.

Dupont, F., **Hannah, C.G.**, **Greenberg, D.A.**, **Cherniawsky, J.Y.** and **Naimie, C.E.** (2002) Modelling System for Tides. *Can. Tech. Rep. Hydrogr. Ocean Sci.*, **221**, vii + 72 pp.

Francois, R.E. and **Garrison G.R.** (1982a) Sound absorption based on ocean measurements: Part I. Pure water and magnesium sulfate contributions. *J. Acoust. Soc. Am.*, **72**, 896–907.

Francois R. E. and **Garrison G. R.** (1982b) Sound absorption based on ocean measurements: Part II. Boric acid contribution and equation for total absorption. *J. Acoust. Soc. Am.*, **72**, 1879–1890.

Gardner, J.V., **Dartnell, P.**, **Mayer, L.A.**, **Hughes Clarke, J.E.**, **Calder, B.R.** and **Duffy, G.** (2005) Shelf-edge deltas and drowned barrier island complexes on the Northwest Florida outer continental shelf. *Geomorphology,* **64**, 133–166.

Greenberg, D.A. (1979) A numerical model investigation of tidal phenomena in the Bay of Fundy and Gulf of Maine. *Mar. Geodesy*, **2**, 161–187.

Hamilton, E.L. and **Bachman, R.T.** (1982) Sound velocity and related properties of marine sediments. *J. Acoust. Soc. Amer.*, **72**, 1891–1904.

Hammerstad, E. (2000) *Backscattering and Seabed Image Reflectivity*. EM Technical Note, Kongsberg Technical Documentation, 5 pp.

Hughes Clarke, J.E. (1994) Toward remote seafloor classification using the angular response of acoustic backscattering: a case study from multiple overlapping GLORIA data. *IEEE J. Ocean. Eng.,* **19,** 364–374.

Hughes Clarke, J.E. (2003) Dynamic motion residuals in swath sonar data: Ironing out the creases. *Int. Hydrogr. Rev.*, **4**, 6–23.

Hughes Clarke, J.E. (2006) Applications of multibeam water column imaging for hydrographic survey. *Hydrogr. J.*, **120**, 3–15.

Hughes Clarke, J.E., Mayer, L.A. and **Wells, D.E.** (1996) Shallow-water imaging multibeam sonars: A new tool for investigating seafloor processes in the coastal zone and on the continental shelf. *Mar. Geophys. Res.*, **18**, 607–629.

Hughes Clarke, J.E., Danforth, B.W. and **Valentine, P.** (1997) Areal Seabed Classification using Backscatter Angular Response at 95 kHz. In: *High Frequency Acoustics in Shallow Water* (Eds N.G. Pace, E. Pouliquen, O. Bergem, and A.P. Lyons). *NATO SACLANTCEN Conf. Proc. Ser.,* **CP-45**, 243–250.

Hughes Clarke, J.E., Gardner, J.V., Torresan, M. and **Mayer, L.A.** (1998) The limits of spatial resolution achievable using a 30kHz multibeam sonar: model predictions and field results. *Proc. OCEANS 98 Conf., Nice,* **3**, 1823–1827.

Hughes Clarke, J.E., Lamplugh, M. and **Kammerer, E.** (2000), Integration of near-continuous sound speed profile information. *Can. Hydrogr. Conf. 2000*, CDROM, 13 pp.

Hughes Clarke, J.E., Dare, P., Beaudoin, J. and **Bartlett, J.** (2005) A stable vertical reference for bathymetric surveying and tidal analysis in the high Arctic. *Proc. US Hydrogr. Conf. 2005*, San Diego, California, 16 pp.

Hughes Clarke, J.E., Iwanowska, K.K., Parrott, D.R., Duffy, G., Lamplugh, M. and **Griffin, J.** (2008) Inter-calibrating multi-source, multi-platform backscatter datasets to assist in compiling regional sediment type maps: Bay of Fundy. *Proc. Can. Hydrogr. Conf. and Nat. Survey. Conf. 2008*, **Paper 8–2,** 22 pp.

Intelmann, S.S., Beaudoin, J. and **Cochrane, G.R.** (2006) Normalization and characterization of multibeam backscatter: Koitlah Point to Point of the Arches, Olympic Coast National Marine Sanctuary - Survey HMPR-115-2004-03. *Marine Sanctuaries Conservation Series MSD-06-03*, US Department of Commerce, National Oceanic and Atmospheric Administration, Marine Sanctuaries Division, Silver Spring, MD, 22 pp.

International Hydrographic Organization (1998) IHO Standards for Hydrographic Surveys, 4thEdn. *Int. Hydrogr. Bur., Spec. Publ.,* **44,** 23 pp.

Iwanowska, K., Hughes Clarke, J.E., Conway, K.W. and **Barrie, V.** (2005) Managing systematic residual errors in multibeam backscatter data. *GEOHAB 2005*, Victoria, Conf. Prog. with abstracts, 80–81.

Jackson, D.R., Winebrenner, D.P. and **Ishimaru, A.** (1986) Application of the composite roughness model to high-frequency bottom backscattering. *J. Acoust. Soc. Am.*, **79**, 1410–1422.

Kammerer, E., Hughes Clarke, J.E., Locat, J., Doucet, N. and **Godin, A.** (1998) Monitoring temporal changes in seabed morphology and composition using multibeam sonars: a case study of the 1996 Saguenay River floods. *Proc. Can. Hydrogr. Conf. 1998*, Victoria, 450–461.

Kongsberg (2005) *EM710 system description*. Kongsberg Maritime Technical Documentation.

Lemoine, F.G., Kenyon, S.C., Factor, J.K., Trimmer, R.G., Pavlis, N.K., Chinn, D. S., Cox, C.M., Klosko, S.M., Luthcke, S.B., Torrence, M.H., Wang, Y.M., Williamson, R.G., Pavlis, E.C., Rapp, R.H. and **Olson, T.R.** (1998) *The Development of the Joint NASA GSFC and NIMA Geopotential Model EGM96*. NASA Goddard Space Flight Center, Greenbelt, Maryland, 20771 USA, NASA/TP-1998-206861.

Llewellyn, K. (2005) *Corrections for Beam Pattern Residuals in Backscatter Imagery from the Kongsberg-Simrad EM300 Multibeam Echosounder.* Unpubl. MScEng Thesis, University of New Brunswick, 105 pp.

Miller, J., Hughes Clarke, J.E. and **Patterson, J.** (1997) How effectively have you covered your bottom? *Hydrogr. J.*, **83**, 3–10.

Milvang, O, Huseby, R.B., Weisteen, K. and **Solberg, A.S.** (1993) Feature extraction from backscatter sonar data. *Acoustic Classification and Mapping of the Seabed. Int. Conf. Proc., 157–164*.

Pace, N.G. and **Dyer, C.M.** (1979) Machine Classification of Sedimentary Sea Bottoms. *IEEE Trans. Geosci. Electron.*, **GE-17**, 52–56.

Pace, N.G. and **Gao, H.** (1988) Swathe Seabed Classification. *IEEE J. Ocean. Eng.,* **13**, 83–90.

Pickrill, R.A and Todd, B.J. (2002) Sea floor mapping on the Scotian Shelf and the Gulf of Maine: implications for the management of ocean resources. *Fishing and Benthic Habitats 2002*, *Symposium on Effects of Fishing Activities on Benthic Habitats: Linking Geology, Biology, Socioeconomics, and Management*, abstracts. Tampa, FL.

Preston, J.M., Christney, A.C., Bloomer, S.F. and **Beaudet, I.L.** (2001) Seabed classification of multibeam sonar images: *MTS/IEEE Oceans 2001 Conf. Proc.*, 2616–2623.

Sonnichsen, G.V., King, T., Jordan, I. and **Li, C.** (2005) Probabilistic analysis of iceberg scouring frequency based on repetitive seabed mapping, offshore Newfoundland and Labrador. *Proc. 18thInt. Conf. Port Ocean Eng. under Arctic Conditions*. POAC'05, Potsdam, NY.

Todd B.J., Fader G.B.J., Courtney R.C. and **Pickrill R.A.** (1999) Quaternary geology and surficial sediment processes, Browns Bank, Scotian Shelf, based on multibeam bathymetry. *Mar. Geol.*, **162,** 165–214.

USACE (2002) Real-Time Kinematic Differential GPS Surveys. In: *Engineering and Design - Hydrographic Surveying, Chapter 16*. US Army Corps of Engineers, EM **1110-2-1003**, 10 pp.

Valentine, P.C. (2005) Sea Floor Image Maps Showing Topography, Sun-Illuminated Topography, Backscatter Intensity, Ruggedness, Slope, and the Distribution of Boulder Ridges and Bedrock Outcrops in the Stellwagen Bank National Marine Sanctuary Region off Boston, Massachusetts. *US Geol. Surv. Sci. Invest. Map* 2840.

Visser H. (2007) OmniSTAR: a DGPS Service for GIS Mapping. *Geomatics World*, March/April, 22–24.

Wilson, J., Gilmour, W. and **Greene, G.** (2005) Mapping fisheries habitat by enhanced multibeam acoustic data in Alaska. *US Hydrogr. Conf. Proc.*, 2005, CDROM.